TABLE 3. RELATIVE RISK FOR RAPID DECLINERS VERSUS SLOW DECLINERS USING LOGISTIC REGRESSION ANALYSES

	%Kco Excluded			Emphysema Scores Excluded		
	Odds Ratio	95% CI	*P* Value	Odds Ratio	95% CI	*P* Value
Emphysema score	1.46	1.01–2.11	0.047			
%Kco, 10%				0.84	0.73–0.96	0.014
Post-bronchodilator FEV_1, % predicted	1.00	0.99–1.02	0.66	1.00	0.99–1.02	0.75
Reversibility of airflow limitation	1.01	0.98–1.05	0.45	1.02	0.98–1.06	0.36
Blood neutrophil count, 100 cells/μl	1.03	1.00–1.07	0.036	1.04	1.01–1.07	0.021
Blood eosinophil count, 10 cells/μl	0.98	0.95–1.01	0.12	0.98	0.95–1.01	0.12
Chronic bronchitis symptom	1.47	0.50–4.36	0.49	1.34	0.44–4.11	0.61
MRC dyspnea scale ⩾2	0.85	0.33–2.23	0.75	0.77	0.30–2.02	0.60
Continuous vs. noncontinuous smokers	0.84	0.35–1.98	0.68	0.70	0.30–1.76	0.42
Exacerbation frequency, events/yr	1.17	0.54–2.54	0.69	1.16	0.54–2.52	0.70
Age, yr	0.99	0.94–1.03	0.52	0.98	0.94–1.03	0.39
Female sex	0.20	0.02–1.67	0.14	0.22	0.03–1.85	0.16

Definition of abbreviations: CI = confidence interval; %Kco = carbon monoxide transfer coefficient (% predicted); MRC = Medical Research Council.

as low as only about 15% in each during the follow-up period because of our intense advice of cessation of smoking before they entered the study. Another reason may be the unique clinical characteristics observed in Japanese patients with COPD, because Japanese subjects participating in the recent UPLIFT study also showed a much smaller annual decline in FEV_1 (27 ml/yr with tiotropium) compared with the overall average (42). It is not clear whether this is caused by ethnic or genetic differences, or by environmental differences, including socioeconomic factors. Another unique finding of this study is the very low incidence of exacerbation during the study period in all subject groups. This was again observed in the Japanese participants in the UPLIFT study and another study only recently published (43). Whatever the reason, the low incidence of exacerbation during the study period may help to elucidate the independent effects of emphysema severity on annual decline in FEV_1 in this study. It is of note that we have seen a dramatic decrease in chronic bronchitis symptoms in patients with COPD for the last two or three decades that certainly contributed low incidence of exacerbation in our population. It may be surprising that we did not see any deleterious effect of continuous smoking on annual decline of FEV_1. We examined the background of the groups classified by smoking behavior (*see* Table E1); however, we could not identify any reasons. The results might be a simple consequence that Rapid decliners were more willing to quit smoking in response to physicians' advice and their worsening symptoms.

It must be noted that a significant proportion of the subjects maintained pulmonary function over a period of 5 years (annual decline, -2 ± 1 ml/yr). Characteristics that significantly discriminate the Sustainers from the others were higher, but within the normal range, levels of eosinophils in blood and more frequent chronic bronchitis symptoms. They had lower levels of emphysema, and slightly but significantly greater BMI. Considering these clinical features, one can speculate that there were some patients with asthma in this group; however, we clinically excluded patients with asthma at entry (Table 1). Furthermore, we did not observe any significant differences in reversibility of airflow limitation among the three groups during the entire follow-up period (*see* Figure E5). Nevertheless, clinicians should pay closer attention to the presence of those patients with COPD who maintain pulmonary function over the long-term in daily practice and future clinical trials.

This study has several limitations. First, most of the subjects were male, and findings may not necessarily be extrapolated to female patients with COPD. This biased sex ratio simply reflects the marked difference in prevalence of smoking between men and women in Japanese society. Second, emphysema severity on CT was visually assessed. However, it was shown that visual emphysema scoring for three CT slices was strongly correlated with objective volume-based computerized assessment for the whole lung in a limited number of subjects (*see* Figure E1). We also found very similar findings (Figure 5), even for those

TABLE 4. RELATIVE RISK FOR SUSTAINERS VERSUS DECLINERS USING LOGISTIC REGRESSION ANALYSES

	%Kco Excluded			Emphysema Scores Excluded		
	Odds Ratio	95% CI	*P* Value	Odds Ratio	95% CI	*P* Value
Emphysema score	0.68	0.47–0.99	0.042			
%Kco, 10%				1.21	1.06–1.38	0.004
Post-bronchodilator FEV_1, % predicted	1.00	0.98–1.01	0.58	1.00	0.98–1.02	0.90
Reversibility of airflow limitation	0.98	0.95–1.01	0.23	0.98	0.94–1.01	0.19
Blood neutrophil count, 100 cells/μl	1.01	0.98–1.04	0.51	1.01	0.98–1.04	0.71
Blood eosinophil count, 10 cells/μl	1.04	1.01–1.06	0.007	1.03	1.01–1.06	0.013
Chronic bronchitis symptom	2.68	1.14–6.30	0.024	2.97	1.24–7.12	0.014
MRC dyspnea scale ⩾2	0.84	0.37–1.91	0.67	0.91	0.39–2.11	0.82
Continuous vs. noncontinuous smokers	0.99	0.48–2.07	0.99	1.23	0.59–2.57	0.58
Exacerbation frequency, events/yr	0.98	0.41–2.34	0.97	1.04	0.43–2.50	0.94
Age, yr	0.97	0.93–1.01	0.13	0.98	0.94–1.02	0.29
Female sex	1.14	0.31–4.20	0.84	1.01	0.27–3.72	0.99

Definition of abbreviations: CI = confidence interval; %Kco = carbon monoxide transfer coefficient (% predicted); MRC = Medical Research Council.

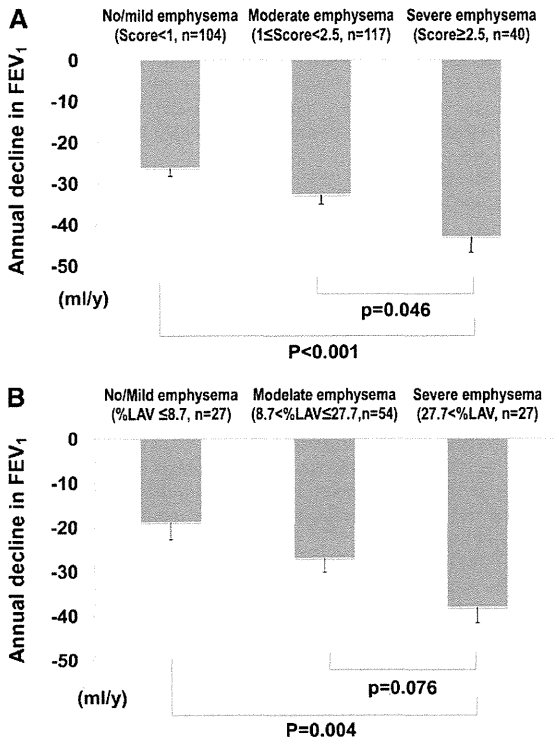

Figure 5. Annual declines in post-bronchodilator FEV_1 among three groups classified by emphysema severity at baseline. Emphysema severity on computer tomography was assessed (*A*) by visual assessment (n = 261) and (*B*) by computerized analysis (n = 108). Subjects with emphysema severity were defined as follows: no or mild emphysema (emphysema score <1, % of low attenuation area [LAA] in the assessed lung <12.5% on average); moderate emphysema (emphysema score <2.5, 12.5% <% of LAA <50%); and severe emphysema (emphysema score <2.5, 50% <% of LAA) (19.) In case of computerized assessment, subjects were classified as no or mild emphysema, less than the 25th percentile; moderate emphysema, the 25th to 75th percentile; and severe emphysema, greater than the 75th percentile of percent low attenuation volume (%LAV). Data show means with SEM.

subjects in whom computerized analysis could be performed. Both K_{CO} and D_{LCO} data are definitely complementary for evaluation of emphysema severity in this study. Finally, the sample size in this study was not so large compared with previous large-scale studies, such as the Lung Health Study (4) and the UPLIFT study (36) in which the rate of annual decline in FEV_1 was also the primary endpoint. Thus, the lack of adequate power as a result of the small sample size may well explain some of the failures in detecting the factors, such as exacerbation and chronic bronchitis syndrome, which would potentially influence natural history of COPD.

In conclusion, we demonstrated that emphysema severity is independently associated with a rapid annual decline in FEV_1 in COPD. We also confirmed the presence of Sustainers who can maintain pulmonary function over a period of 5 years provided that they receive appropriate therapy. Emphysema severity and presence of Sustainers should thus be considered in daily practice and in future clinical trials where annual decline in FEV_1 is a primary outcome measurement.

Author disclosures are available with the text of this article at www.atsjournals.org.

Hokkaido COPD Cohort Study Group Investigators: Yoshikazu Kawakami, Youichi Nishiura, Hiroshi Saito, Tetsuya Kojima, Kazuhiko Sakai, Yoriko Demura, Yukihiro Tsuchida, Motoko Tsubono, Kazuhiro Tsuboya, and Shinichi Kakimoto, KKR Sapporo Medical Center; Kiyonobu Kimura, Ikuo Nakano, Moto Katabami, Kouichi Itabashi, Kiyoshi Morikawa, Seiichi Tagami, Yoshihiro Otsuka, Rika Sato, Junichiro Kojima, Shinji Nigawara, Takashi Morioka, Ichiro Sakai, Shiro Fujii, Kazuyoshi Kanehira, Ryota Funakoshi, Yui Takashima, Masahiro Awaka, Hitoshi Ishii, Makoto Nakayama, Hiroki Honda, Ryo Kaneda, and Masahisa Takagi, Hokkaido Chuo Rosai Hospital; Hiroshi Yamamoto, Kenji Akie, Fumihiro Honmura, Shinichi Kusudou, Hiroshi Izumi, Kensuke Baba, Hiroki Goya, Kihoko Kitamura, Shiho Mineta, Takayo Takeda, Kiyoshi Kubo, Junko Yamaguchi, and Hiroshi Nara, Sapporo City General Hospital; Tsuyoshi Nakano, Chihiro Naka, Hiroko Sato, Teiji Yamamoto, Toshio Abe, and Nobuo Tomita, Otaru City Hospital; Kimihiro Takeyabu, Yuji Ootsuka, and Naoki Watanabe, Otaru Kyokai Hospital; Fujiya Kishi, Akihide Ito, Michihiro Fujino, Masashi Ohe, Toshiyuki Harada, Yasuko Noda, Teruyo Takahashi, Keiko Abe, Akira Nakajima, Tomonori Fujii, Hiroshige Mori, Hideo Taguchi, Takashi Kojima, Ryouji Minami, Shigeki Murakami, Yuzuri Oono, Osamu Ishigamori, Satoru Akimoto, Takashi Emoto, Daichi Takahashi, and Risa Ajioka, Hokkaido Social Insurance Hospital; Akira Kamimura, Nobuyuki Hakuma, Noriaki Sukou, Eriko Anada, Tamaki Numata, Teiko Itakura, Tomoko Iizawa, Rina Ohya, and Yoshihiro Honoki, Iwamizawa City General Hospital; Kazuo Takaoka, Isamu Doi, Miki Suzuki, Sachiko Komuro, Yoshiko Yoshida, Michiko Kobayashi, and Hitoshi Seki, Sapporo Social Insurance General Hospital; Atsushi Ishimine, Ryouji Nakano, Masako Ishihara, Fumiyo Itagaki, Naoya Matsuzaka, Takae Kosukegawa, Eriko Miyajima, Kimitsugu Nakamura, Wako Funayama, Katsumigi Tsuchiya, and Ryouji Kaihatsu, Kinikyo Chuo Hospital; Kaoru Kamishima and Yasushi Hasegawa, Tenshi Hospital; Kunio Hamada, Yoko Ito, Motoko Kobayashi, Takeshi Hosokawa, Nao Odajima, Chinatsu Moriyama, Takayuki Yoshida, Takashi Inomata, Kanako Maki, Eiji Shibuya, Yoshiko Obata, Kotomi Hosono, Kana Yoshikuni, and Tomoko Akiyama, First Department of Medicine/Hokkaido University School of Medicine; Yuya Onodera, Department of Radiology, Hokkaido University Graduate School of Medicine; Tsukasa Sasaki, Division of Radiology, Department of Diagnosis and Treatment Support Part, Hokkaido University Hospital; Katsuaki Nitta, Masafumi Yamamoto, and Shigetaka Mizuno, Division of Pulmonary Function, Department of Laboratory Medicine, Hokkaido University Hospital; Kenji Miyamoto, Division of Rehabilitation Science, Faculty of Health Sciences, Hokkaido University; and Nobuyuki Hizawa, Pulmonology, Doctoral Program in Clinical Science, Graduate School of Comprehensive Human Sciences, University of Tsukuba.

Acknowledgment: The authors thank Hideka Ashikaga, Ayako Kondo, and Yuko Takagi at the Central Office of Hokkaido COPD Cohort Study; the staff of Exam Co., Ltd.; Tatsuo Kagimura at the Medical Data Services Department Biostatistics Group in Nippon Boehringer Ingelheim; Takahiro Nakamura; Masaki Minami at the Medical Affairs Department Respiratory and Allergy Group in Nippon Boehringer Ingelheim; and the medical doctors, nurses, and technicians in all hospitals involved in the study.

References

1. Roisin RR. Global strategy for the diagnosis, management and prevention of COPD updated 2009 [accessed 2010 April 28]. Available from: http://www.goldcopd.com
2. Wise RA. The value of forced expiratory volume in 1 second decline in the assessment of chronic obstructive pulmonary disease progression. *Am J Med* 2006;119:4–11.
3. Anthonisen NR, Connett JE, Kiley JP, Altose MD, Bailey WC, Buist AS, Conway A Jr, Enright PL, Kanner RE, O'Hara P, *et al.* Effects of smoking intervention and the use of an inhaled anticholinergic bronchodilator on the rate of decline of FEV1. The Lung Health Study. *JAMA* 1994;272:1497–1505.
4. Scanlon PD, Connett JE, Waller LA, Altose MD, Bailey WC, Buist AS. Smoking cessation and lung function in mild-to moderate chronic obstructive pulmonary disease. The Lung Health Study. *Am J Respir Crit Care Med* 2000;161:381–390.
5. Donaldson GC, Seemungal TA, Bhowmik A, Wedzicha JA. Relationship between exacerbation frequency and lung function decline in chronic obstructive pulmonary disease. *Thorax* 2002;57:847–852. [Published erratum appears in *Thorax* 2008;63:753.]
6. Decramer M, Celli B, Kesten S, Lystig T, Mehra S, Tashkin DP; UPLIFT Investigators. Effect of tiotropium on outcomes in patients with moderate chronic obstructive pulmonary disease (UPLIFT): a prespecified subgroup analysis of a randomised controlled trial. *Lancet* 2009;374: 1171–1178.
7. Celli BR, Thomas NE, Anderson JA, Ferguson GT, Jenkins CR, Jones PW, Vestbo J, Knobil K, Yates JC, Calverley PM. Effect of pharmacotherapy on rate of decline of lung function in chronic obstructive pulmonary disease: results from the TORCH study. *Am J Respir Crit Care Med* 2008;178:332–338.
8. Hogg JC. Pathophysiology of airflow limitation in chronic obstructive pulmonary disease. *Lancet* 2004;364:709–721.
9. Remy-Jardin M, Edme JL, Boulenguez C, Remy J, Mastora I, Sobaszek A. Longitudinal follow-up study of smoker's lung with thin-section

CT in correlation with pulmonary function tests. *Radiology* 2002;222: 261–270.
10. Yuan R, Hogg JC, Paré PD, Sin DD, Wong JC, Nakano Y, McWilliams AM, Lam S, Coxson HO. Prediction of the rate of decline in FEV(1) in smokers using quantitative computed tomography. *Thorax* 2009;64: 944–949.
11. Hoesein M FA, de Hoop B, Zanen P, Gietema H, Kruitwagen CL, van Ginneken B, Isgum I, Mol C, van Klaveren RJ, Dijkstra AE, *et al.* CT-quantified emphysema in male heavy smokers: association with lung function decline. *Thorax* 2011;66:782–787.
12. Haruna A, Muro S, Nakano Y, Ohara T, Hoshino Y, Ogawa E, Hirai T, Niimi A, Nishimura K, Chin K, *et al.* CT scan findings of emphysema predict mortality in COPD. *Chest* 2010;138:635–640.
13. Ohara T, Hirai T, Muro S, Haruna A, Terada K, Kinose D, Marumo S, Ogawa E, Hoshino Y, Niimi A, *et al.* Relationship between pulmonary emphysema and osteoporosis assessed by CT in patients with COPD. *Chest* 2008;134:1244–1249.
14. Bon J, Fuhrman CR, Weissfeld JL, Duncan SR, Branch RA, Chang CC, Zhang Y, Leader JK, Gur D, Greenspan SL, *et al.* Radiographic emphysema predicts low bone mineral density in a tobacco-exposed cohort. *Am J Respir Crit Care Med* 2011;183:885–890.
15. McAllister DA, Maclay JD, Mills NL, Mair G, Miller J, Anderson D, Newby DE, Murchison JT, Macnee W. Arterial stiffness is independently associated with emphysema severity in patients with chronic obstructive pulmonary disease. *Am J Respir Crit Care Med* 2007;176:1208–1214.
16. Wilson DO, Weissfeld JL, Balkan A, Schragin JG, Fuhrman CR, Fisher SN, Wilson J, Leader JK, Siegfried JM, Shapiro SD, *et al.* Association of radiographic emphysema and airflow obstruction with lung cancer. *Am J Respir Crit Care Med* 2008;178:738–744.
17. Han MK, Agusti A, Calverley PM, Celli BR, Criner G, Curtis JL, Fabbri LM, Goldin JG, Jones PW, Macnee W, *et al.* Chronic obstructive pulmonary disease phenotypes: the future of COPD. *Am J Respir Crit Care Med* 2010;182:598–604.
18. Agusti A, Calverley PM, Celli B, Coxson HO, Edwards LD, Lomas DA, MacNee W, Miller BE, Rennard S, Silverman EK, *et al*; Evaluation of COPD Longitudinally to Identify Predictive Surrogate Endpoints (ECLIPSE) investigators. Characterisation of COPD heterogeneity in the ECLIPSE cohort. *Respir Res* 2010;11:122.
19. Makita H, Nasuhara Y, Nagai K, Ito Y, Hasegawa M, Betsuyaku T, Onodera Y, Hizawa N, Nishimura M; Hokkaido COPD Cohort Study Group. Characterisation of phenotypes based on severity of emphysema in chronic obstructive pulmonary disease. *Thorax* 2007;62:932–937.
20. Müller NL, Staples CA, Miller RR, Abboud RT. Density mask: an objective method to quantitate emphysema using computed tomography. *Chest* 1988;94:782–787.
21. Newell JD Jr, Quantitative computed tomography of lung parenchyma in chronic obstructive pulmonary disease: an overview. *Proc Am Thorac Soc* 2008;5:915–918.
22. Dowson LJ, Guest PJ, Stockley RA. Longitudinal changes in physiological, radiological, and health status measurements in alpha(1)-antitrypsin deficiency and factors associated with decline. *Am J Respir Crit Care Med* 2001;164:1805–1809.
23. Thurlbeck WM, Wright JL. Emphysema: clinical and clinicopathologic correlations, radiographic alterations, lung reduction surgery. In: Decker BC, editor. Thurlbeck's chronic airflow obstruction. London: Hamilton; 1999. pp. 189–222.
24. Annual decline of forced expiratory volume in 1 sec (FEV_1) over 4 years in COPD based on clinical phenotypes [abstract]. *Am J Respir Crit Care Med* 2010;181:A1534.
25. Donaldson GC, Wedzicha JA. COPD exacerbations. 1: Epidemiology. *Thorax* 2006;61:164–168.
26. Jones PW, Quirk FH, Baveystock CM, Littlejohns P. A self-complete measure of health status for chronic airflow limitation. The St. George's Respiratory Questionnaire. *Am Rev Respir Dis* 1992;145:1321–1327.
27. American Thoracic Society. Single-breath carbon monoxide diffusing capacity (transfer factor). Recommendations for a standard technique—1995 update. *Am J Respir Crit Care Med* 1995;152:2185–2198.
28. Committee of Respiratory Physiology in Japanese Respiratory Society [Guideline of respiratory function tests–spirometry, flow-volume curve, diffusion capacity of the lung]. *Nihon Kokyuki Gakkai Zasshi* 2004;1–56.
29. Konno S, Makita H, Hasegawa M, Nasuhara Y, Nagai Katsura, Betsuyaku T, Hizawa N, Nishimura M. Beta2-adrenergic receptor polymorphisms as a determinant of preferential bronchodilator responses to b2-agonist and anticholinergic agents in Japanese patients with chronic obstructive pulmonary disease. *Pharmacogenet Genomics* 2011;21:687–693.
30. Goddard PR, Nicholson EM, Laszlo G, Watt I. Computed tomography in pulmonary emphysema. *Clin Radiol* 1982;33:379–387.
31. Park KJ, Bergin CJ, Clausen JL. Quantitation of emphysema with three-dimensional CT densitometry: comparison with two-dimensional analysis, visual emphysema scores, and pulmonary function test results. *Radiology* 1999;211:541–547.
32. Madani A, Zanen J, de Maertelaer V, Gevenois PA. Pulmonary emphysema: objective quantification at multi-detector row CT: comparison with macroscopic and microscopic morphometry. *Radiology* 2006;238:1036–1043.
33. Littell RC, Milliken GA, Stroup WW, Wolfinger RD, Schabenberger O. SAS for mixed models, 2nd ed. Cary, NC: SAS Institute Inc.; 2006.
34. Stokes ME, Davis CS, Koch GG. Categorical data analysis using the SAS System, 2nd ed. Cary, NC: SAS Institute Inc.; 2000.
35. Burrows B. An overview of obstructive lung diseases. *Med Clin North Am* 1981;65:455–471.
36. Tashkin DP, Celli B, Senn S, Burkhart D, Kesten S, Menjoge S, Decramer M; UPLIFT Study Investigators. UPLIFT Study Investigators. A 4-year trial of tiotropium in chronic obstructive pulmonary disease. *N Engl J Med* 2008;359:1543–1554.
37. Calverley PM, Anderson JA, Celli B, Ferguson GT, Jenkins C, Jones PW, Yates JC, Vestbo J; TORCH investigators. Salmeterol and fluticasone propionate and survival in chronic obstructive pulmonary disease. *N Engl J Med* 2007;356:775–789.
38. Patel BD, Coxson HO, Pillai SG, Agustí AG, Calverley PM, Donner CF, Make BJ, Müller NL, Rennard SI, Vestbo J, *et al*; International COPD Genetics Network. Airway wall thickening and emphysema show independent familial aggregation in chronic obstructive pulmonary disease. *Am J Respir Crit Care Med* 2008;178:500–505.
39. Ito I, Nagai S, Handa T, Muro S, Hirai T, Tsukino M, Mishima M. Matrix metalloproteinase-9 promoter polymorphism associated with upper lung dominant emphysema. *Am J Respir Crit Care Med* 2005; 172:1378–1382.
40. Hizawa N, Makita H, Nasuhara Y, Hasegawa M, Nagai K, Ito Y, Betsuyaku T, Konno S, Nishimura M; Hokkaido COPD Cohort Study Group. Functional single nucleotide polymorphisms of the CCL5 gene and nonemphysematous phenotype in COPD patients. *Eur Respir J* 2008;32: 372–378.
41. Martinez FJ, Foster G, Curtis JL, Criner G, Weinmann G, Fishman A, DeCamp MM, Benditt J, Sciurba F, Make B, *et al*; NETT Research Group. Predictors of mortality in patients with emphysema and severe airflow obstruction. *Am J Respir Crit Care Med* 2006;173:1326–1334.
42. Fukuchi Y, Fernandez L, Kuo HP, Mahayiddin A, Celli B, Decramer M, Kesten S, Liu D, Tashkin D. Efficacy of tiotropium in COPD patients from Asia: a subgroup analysis from the UPLIFT trial. *Respirology* 2011;16:825–835.
43. Tanabe N, Muro S, Hirai T, Oguma T, Terada K, Marumo S, Kinose D, Ogawa E, Hoshino Y, Mishima M. Impact of exacerbations on emphysema progression in chronic obstructive pulmonary disease. *Am J Respir Crit Care Med* 2011;183:1653–1659.

Bone 50 (2012) 1123–1129

Contents lists available at SciVerse ScienceDirect

Bone

journal homepage: www.elsevier.com/locate/bone

Original Full Length Article

A clinical study of alveolar bone tissue engineering with cultured autogenous periosteal cells: Coordinated activation of bone formation and resorption

Masaki Nagata [a,*], Hideyuki Hoshina [b], Minqi Li [c,d], Megumi Arasawa [a], Kohya Uematsu [a], Shin Ogawa [a], Kazuho Yamada [b], Tomoyuki Kawase [e], Kenji Suzuki [f], Akira Ogose [g], Ichiro Fuse [h], Kazuhiro Okuda [i], Katsumi Uoshima [b], Koh Nakata [j], Hiromasa Yoshie [i], Ritsuo Takagi [a]

[a] Department of Oral and Maxillofacial Surgery, Niigata University Graduate School of Medical and Dental Sciences, 2–5274 Gakkocho-dori, Chuo-ku, Niigata 951–8514, Japan
[b] Oral Implant Clinic, Niigata University Medical and Dental Hospital, 754 Asahimachi-dori, Ichiban-cho, Chuo-ku, Niigata 951–8520, Japan
[c] Department of Bone Metabolism, The School of Stomatology, Shandong University, Wenhua West Road 44-1, Jinan 250012, China
[d] Department of Developmental Biology of Hard Tissue, Graduate School of dental Medicine, Hokkaido University, Kita 13 Nishi 7 Kita-ku, Sapporo 060–8586, Japan
[e] Division of Oral Bioengineering, Department of Tissue Regeneration and Reconstitution, Niigata University Graduate School of Medical and Dental Sciences, 2–5274 Gakkocho-dori, Chuo-ku, Niigata 951–8514, Japan
[f] Department of Gastroenterology and Hepatology, Niigata University Graduate School of Medical and Dental Sciences, 757–1 Asahimachi-dori Ichiban-cho, Chuo-ku, Niigata 951–8510, Japan
[g] Division of Orthopaedic Surgery, Department of Regenerative Transplant Medicine, Niigata University Graduate School of Medical and Dental Sciences, 757–1 Asahimachi-dori Ichiban-cho, Chuo-ku, Niigata 951–8510, Japan
[h] Department of Hematology, Niigata University Graduate School of Medical and Dental Sciences, 757–1 Asahimachi-dori, Ichiban-cho, Chuo-ku, Niigata 951–8510, Japan
[i] Division of Periodontology, Department of Oral Biological Science, Niigata University Graduate School of Medical and Dental Sciences, 2–5274 Gakkocho-dori, Chuo-ku, Niigata 951–8514, Japan
[j] Bioscience Medical Research Center, Niigata University Medical and Dental Hospital, 754 Asahimachi-dori Ichiban-cho, Chuo-ku, Niigata 951–8520, Japan

ARTICLE INFO

Article history:
Received 14 October 2011
Revised 16 February 2012
Accepted 23 February 2012
Available online 2 March 2012

Edited by: Robert Recker

Keywords:
Clinical study
Cultured autogenous periosteal cell
Alveolar bone
Bone tissue engineering
Three-dimensional computed tomography
Dental implant

ABSTRACT

In ongoing clinical research into the use of cultured autogenous periosteal cells (CAPCs) in alveolar bone regeneration, CAPCs were grafted into 33 sites (15 for alveolar ridge augmentation and 18 for maxillary sinus lift) in 25 cases. CAPCs were cultured for 6 weeks, mixed with particulate autogenous bone and platelet-rich plasma, and then grafted into the sites. Clinical outcomes were determined from high-resolution three-dimensional computed tomography (3D-CT) images and histological findings. No serious adverse events were attributable to the use of grafted CAPCs. Bone regeneration was satisfactory even in cases of advanced atrophy of the alveolar process. Bone biopsy after bone grafting with CAPCs revealed prominent recruitment of osteoblasts and osteoclasts accompanied by angiogenesis around the regenerated bone. 3D-CT imaging suggested that remodeling of the grafted autogenous cortical bone particles was faster in bone grafting with CAPCs than in conventional bone grafting. The use of CAPCs offers cell-based bone regeneration therapy, affording complex bone regeneration across a wide area, and thus expanding the indications for dental implants. Also, it enables the content of particulate autogenous bone in the graft material to be reduced to as low as 40%, making the procedure less invasive, or enabling larger amounts of graft materials to be prepared. It may also be possible to dispense with the use of autogenous bone altogether in the future. The results suggest that CAPC grafting induces bone remodeling, thereby enhancing osseointegration and consequently reducing postoperative waiting time after dental implant placement.

Introduction

Diseases affecting the maxillofacial region often cause defects in alveolar or gnathic bone. The maxillofacial bones are an important determinant of facial features and play a pivotal role in mastication and articulation. Thus, rehabilitation therapy that helps morphological and functional recovery of the maxillofacial bones is an important component of the strategies required after the diseases have been treated. Autogenous bone grafting is the most realistic and effective method for regenerating bone tissue in defect sites and is therefore widely used. However, the bone harvesting that is needed to prepare graft materials is accompanied by donor site morbidity such as pain

Abbreviations: ALP, Alkaline phosphatase; CAPC, Cultured autogenous periosteal cell; SL, Maxillary sinus lift; PRP, Platelet rich plasma; TRAP, Tartrate-resistant acid phosphatase; 3D-CT image, three-dimensional CT image.

* Corresponding author. Fax: +81 25 223 5792.
E-mail addresses: nagata@dent.niigata-u.ac.jp (M. Nagata), hoshina@dent.niigata-u.ac.jp (H. Hoshina), liminqi@den.hokudai.ac.jp (M. Li), megumia@dent.niigata-u.ac.jp (M. Arasawa), ue@dent.niigata-u.ac.jp (K. Uematsu), shin@dent.niigata-u.ac.jp (S. Ogawa), kazuho@dent.niigata-u.ac.jp (K. Yamada), kawase@dent.niigata-u.ac.jp (T. Kawase), kjsuzuki@med.niigata-u.ac.jp (K. Suzuki), aogose@med.niigata-u.ac.jp (A. Ogose), fuse@med.niigata-u.ac.jp (I. Fuse), okuda@dent.niigata-u.ac.jp (K. Okuda), fish@dent.niigata-u.ac.jp (K. Uoshima), radical@med.niigata-u.ac.jp (K. Nakata), yoshie@dent.niigata-u.ac.jp (H. Yoshie), takagi@dent.niigata-u.ac.jp (R. Takagi).

8756-3282/$ – see front matter © 2012 Elsevier Inc. All rights reserved.
doi:10.1016/j.bone.2012.02.631

and increased risk of infection, and such morbidity itself sometimes extends the duration of treatment.

To improve the effectiveness of bone tissue engineering, bone graft substitutes, growth factors, and cell-based approaches have been tested. Calcium phosphate-based materials are the most widely used bone graft substitutes, but their efficacy in restoring the maxillofacial region remains unclear; consequently, the host sites and grafting amounts should be carefully evaluated before use. The efficacy of bone morphogenetic proteins (BMPs) in bone regeneration has been well documented in animal models as well as clinical studies. However, their actual clinical use is still limited. The high costs of BMP-2 and BMP-7 formulations may, at least in part, explain the limited indications for BMP therapy [1,2]. Another well-studied growth factor related to osteoinductive activity is fibroblast growth factor 2 (FGF2). It was experimentally revealed that sustained release of FGF2 induces bone regeneration via a mechanism that activates the proliferation and differentiation of periosteal cells around the bone [3]. A clinical study of FGF2 for treating bone in the oral region is ongoing [4], and will hopefully lead to clinical application of FGF2 in alveolar bone regeneration in the near future. Although it is convenient to use growth factor formulations in clinics, a disadvantage is that growth factor administration cannot promote bone regeneration in a wide area.

In cell-based regenerative therapy, grafted cells supply the cell population responsible for tissue regeneration and also serve as growth factor producers. With this in mind, cell-based regenerative therapy is expected to allow for the regeneration of tissues with low regenerative potential. After examining existing studies, reported by our group and others [3,5–10], in our search for a new approach to bone regeneration in a wide area in the maxillofacial region, we have developed a tissue-engineering approach aided by the administration of cells derived from autogenous periosteum. Compared to highly pluripotent mesenchymal stromal cells (MSCs) [11,12], periosteum and periodontium contain more cells that are committed to bone tissue maintenance. So, it is noteworthy that these cells provide osteoblasts responsible for bone formation, and also can promote favorable regeneration of blood vessels and nerve filaments and the recruitment of cells responsible for bone resorption [13,14]. In addition, the periosteum is freely accessible via the superficial layer in the oral cavity throughout the life span, and this is another important advantage of using periosteum. In this study, we examine the treatment outcomes of 25 patients who underwent autogenous bone grafting with CAPCs at our institute, and discuss the effects and principles of this cell therapy in bone regenerative medicine.

Materials and methods

Patients

From among 40 patients scheduled to undergo alveolar bone augmentation prior to dental implant placement between April 2007 to July 2011, 25 patients without major organ failure, metabolic disorder, or infectious disease provided informed consent to participate in this preliminary clinical study of alveolar bone engineering with administration of CAPCs. The remaining 15 patients who underwent conventional bone grafting, because either they did not consent to the use of CAPCs or the procedure could not be undertaken due to time constraints or a failure of CAPC culture, served as the reference group and were examined by morphometric analysis and biopsy.

The study protocol was approved by the Institutional Review Board of the Niigata University Medical and Dental Hospital. The work described here was carried out in accordance with The Code of Ethics of the World Medical Association (Declaration of Helsinki) for experiments involving humans.

Cultivation of periosteum

CAPCs were prepared in the bioclean room of the Cell Processing Center of Niigata University Medical and Dental Hospital, following the method described previously [7]. Briefly, periosteum samples (50 mm^2, 5×10 mm) were harvested from the molar region of the mandible under local anesthesia. Small pieces of the periosteum specimen were placed directly onto 100 mm culture dishes with culture medium (Medium 199 with Earle's salts, Invitrogen, Carlsbad, CA) containing 10% fetal bovine serum (sourced in New Zealand, SAFC Bioscience, Inc., Tokyo, Japan), 25 mg ascorbic acid (Sigma Chemical, St. Louis, MO), 100 IU/ml penicillin (Invitrogen), 100 μg/ml streptomycin (Invitrogen), and 250 ng/ml amphotericin B (Invitrogen) and incubated at 37 °C in an atmosphere of 10% CO_2. Culture medium was changed every 3 days. Periosteum samples were incubated for around 6 weeks until the cells formed a sheet. All equipment and procedures involved in the production of the CAPC sheet were maintained in accordance with the Standard Operating Procedures of our institute observing Good Manufacturing Practices.

Preparation of graft materials and grafting procedure

Two hundred milliliters of whole blood was collected into a citrate-containing blood bag (Terumo, Tokyo, Japan), and centrifuged at 1320×*g* for 3 min. The resulting plasma was further centrifuged at 2690×g for 4 min to obtain 30 ml of platelet-rich plasma (PRP). Because of the wide variance in blood composition, the eventual platelet count of PRPs varied around 80–200×10^4 μl, approximately 4- to 6-fold above the physiological level which is considered to be the platelet concentration required for a positive PRP effect on tissue regeneration [15]. CAPC sheet fragments were mixed with PRP and particulate autogenous bone, and then with 2% $CaCl_2$ (0.15 to 0.2 volume of PRP) to obtain a glue-like graft material in a few minutes [16] (Fig. 1). The amount of PRPs mixed was five to six times that of the bone weight of the grafts, but the composition of graft materials could not be strictly controlled due to differences in the amounts of harvested bone and CAPC sheets generated and also because of PRP glue formation. Types of grafting procedures and the composition and amounts of graft materials used in individual cases are summarized in Table 1.

Three-dimensional analysis of augmented bone

CT scans of the maxillary sinus region were performed before treatment and at 3 months (3 M) and 1 year (1Y) after sinus floor lift. Scans were carried out using 64-multidetector CT (Aquillon, Toshiba, Tokyo, Japan) and data were acquired under the following protocol: 0.5 mm slice thickness, 0.3 mm slice interval, and 21 helical pitch. A total of 21 images were analyzed for 4 bone grafts with CAPCs and 3 conventional bone grafts for maxillary sinus lift (SL).

Three-dimensional (3D) images of the maxilla taken before treatment and at 3 M and 1Y were constructed from DICOM data. The images were adjusted and unified by superimposing the coordinates on anatomical landmarks using Real INTAGE (Cybernet Systems, Tokyo, Japan). Color mapping of the images was applied to identify bone quality according to the classification based on bone density as determined by Hounsfield units (HU) as follows: D1: >1250 HU; D2: 850–1250 HU; D3: 350–850 HU; D4: 150–350 HU; and D5: <50–150 HU [17].

Volumetric measurement of the augmented bone was obtained from DICOM data by Real INTAGE (Cybernet Systems). Data were transformed into isotropic voxel size and augmented bone volume was calculated from voxel number in the extracted images: HU >50 as the total volume or <850 HU and >850 HU as volumetric categories. Volume changes were calculated as ratios of the augmented bone volumes at 1Y to 3 M after the graft.

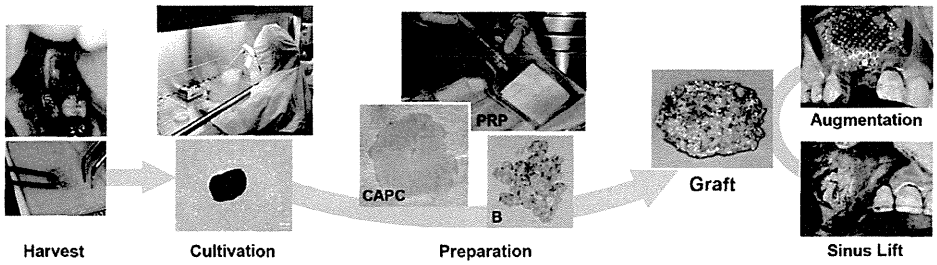

Fig. 1. Procedure of autogenous bone grafting with cultured autogenous periosteal cells (CAPCs). Periosteum specimens were harvested from the bone surface of the mandibular molar region. While culturing in the bioclean room, cells derived from the periosteum started to grow around the periosteum pieces, and then proliferated to form a multi-layer CAPC sheet. The CAPC sheet cultured to the size of 3–4 cm were blended with particulate autogenous bone (B), and then made into glue-like materials by mixing with PRP. The resulting grafting materials were used for alveolar ridge augmentation or maxillary sinus lift.

Histological and histomorphometric analyses

Four months after the graft, biopsies were obtained from the implant sites. The biopsy specimens were placed in 10% formaldehyde, followed by decalcification in 3% EDTA for 4 weeks. Then, 8-μm paraffin sections were used for H-E staining, alkaline phosphatase (ALP) immunohistochemistry, and tartrate-resistant acid phosphatase (TRAP) enzyme histochemistry [18]. For ALP-TRAP double staining, deparaffinized sections were treated with 0.1% hydrogen peroxidase for 15 min to inhibit endogenous peroxidase, and preincubated with 1% bovine serum albumin in phosphate-buffered saline for 30 min at room temperature. Antisera against tissue nonspecific ALP [19] were applied to the sections at a dilution of 1:200 overnight at 4 °C. Sections were then incubated with horseradish peroxidase-conjugated goat anti-rabbit IgG (Chemicon International Inc., Temecula, CA). Immune complexes were visualized using diaminobenzidine staining. Then, the TRAP activity was detected by incubating with a mixture of 2.5 mg naphthol AS-BI phosphate (Sigma), 18 mg red violet LB salt (Sigma), and 100 mM L (+) tartaric acid (0.76 g; Sigma) diluted in 0.1 M sodium acetate buffer (pH 5.0) for 15 min at 37 °C. The sections were counterstained faintly with methyl green.

The gross cross-sectional area of ALP-positive sites (shown in dark-brown) in the $870 \times 650\ \mu m^2$ square view was histomorphometrically analyzed using image analysis software (WinROOF, Mitani Corp., Fukui, Japan). In brief, after RGB separation and manually adjusting threshold, images were binarized, and the ALP-positive area was calculated as a percentage of the whole square view area. TRAP-positive cells were counted per $870 \times 650\ \mu m^2$ square view.

Results

CAPCs promoted good bone regeneration and reduced the amounts of bone required for harvesting

Autologous bone grafting with CAPCs was performed at a total of 33 sites (15 for alveolar ridge augmentation and 18 for maxillary SL) in 25 patients. The bone was harvested from the anterior region of the mandibular ramus in the majority of cases and from the iliac crest in one case. Bone regeneration after autogenous bone grafting

Table 1
Summary of grafting procedures and composition of graft materials used in individual cases.

Case #	Age	Sex	Method	Host site	Doner site	Bone (%)	Cultured periosteal cells (%)	PRP glue (%)	Total graft (g)	Findings
1	59	M	SL	Maxillary sinus	Mandible	79	10	11	5.6	
2	56	M	SL	Maxillary sinus	Mandible	73	8	19	6.6	Atrophic sinus floor <2 mm
3	52	F	SL + Aug	Maxillary sinus + molar	Mandible	36	23	41	7.0	Sinusitis, progressive bone resorption
4	18	M	Aug	Maxillary front	Mandible	35	23	42	3.0	
5	52	F	SL	Maxillary sinus	Mandible	24	28	49	4.0	
6	60	F	Aug	Maxillary front	Mandible	55	36	9	2.2	
7	61	F	Aug	Mandibular molar	Mandible	26	55	19	0.7	
8	56	F	SL	Maxillary sinus	Mandible	74	13	13	3.8	
9	63	F	Aug	Mandibular molar	Mandible	61	25	14	2.8	Partial exposure of Ti-Mesh
10	57	M	SL + Aug	Maxillary sinus + molar	Mandible	60	11	29	5.5	Atrophic sinus floor <2 mm
11	62	F	SL	Maxillary sinus	Mandible	55	17	28	5.5	Atrophic sinus floor <2 mm
12	57	F	SL	Maxillary sinus	Mandible	46	25	30	2.9	
13	72	F	SL	Bilateral maxillary sinuses	Iliac crest	85	9	7	6.9	Atrophic sinus floor <2 mm
14	45	M	Aug	Maxillary front	Mandible	44	25	31	4.0	
15	48	M	Aug	Mandibular molar	Mandible	46	9	45	3.7	
16	45	M	SL + Aug	Maxillary sinus + molar	Mandible	58	17	25	6.0	
17	70	M	SL + Aug	Bilateral maxillary sinuses + mandibular molar	Mandible	71	10	18	8.2	Atrophic sinus floor <2 mm
18	76	M	Aug	Mandibular molar	Mandible	40	37	23	1.5	Partial fibrosis of graft
19	52	F	Aug	Maxillary front	Mandible	38	24	38	2.1	
20	65	F	SL	Maxillary sinus	Mandible	40	37	23	3.0	Atrophic sinus floor <2 mm
21	52	M	Aug	Bilateral mandibular molar	Mandible	53	13	35	4.0	
22	68	M	SL	Maxillary sinus	Mandible	52	8	40	5.2	Atrophic sinus floor <2 mm
23	28	F	Aug	Maxlilary front-molar	Mandible	20	35	45	2.0	
24	57	F	SL	Maxillary sinus	Mandible	48	13	38	6.0	Atrophic sinus floor <2 mm
25	59	M	SL	Bilateral maxillary sinuses	Mandible	54	6	40	7.4	Atrophic sinus floor <2 mm

Aug: alveolar augmentation, SL: sinus lift, PRP glue: platelet-rich plasma glue, Ti-mesh: titanium mesh, (%): weight percentage, (g): weight in grams.

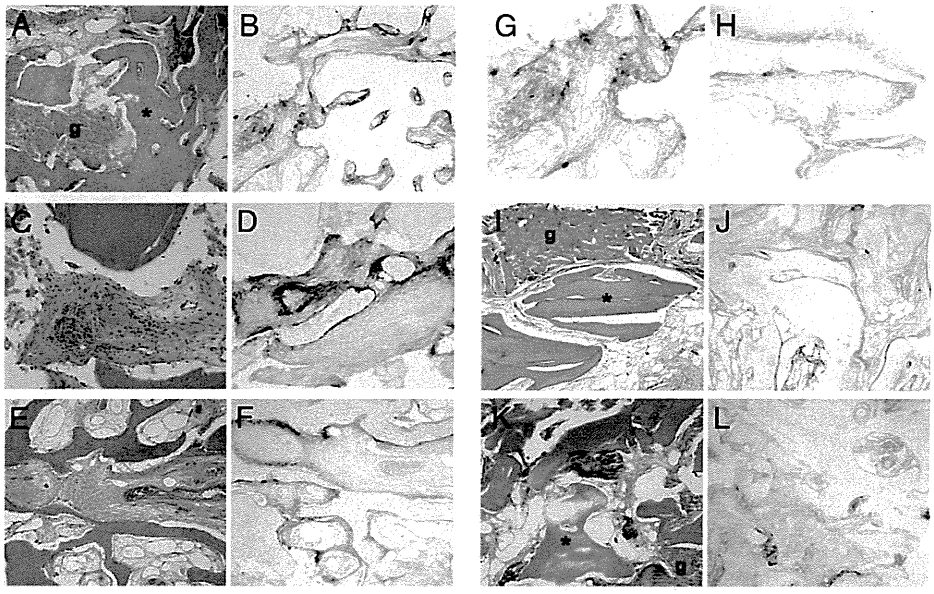

Fig. 2. Histological analysis of biopsy specimens recovered from the recipient sites at 4 months after bone grafting with CAPCs (A–H) or conventional bone grafting (I–L). A, C, E (H–E staining) and B, D, F, G, H (ALP-TRAP double staining): Active new-bone formation was observed in specimens recovered from the site of a bone graft with CAPCs. (A) Newly formed bone tissue surrounds the grafted particulate autogenous bone. (C) Deposition of the bone matrix is apparent inside the accumulated periosteal cell-like cells, which are similar to those observed during intramembranous bone formation. (B, D, F) Cells strongly immunopositive for ALP activity are distributed around the newly formed bone, and (C and E) blood vessels were often observed. G and H (enlarged images of B and F, respectively) show distribution of cells positive for TRAP activity (red) on the surface of the newly formed bone and grafted bone particles. I, K (H-E staining) and J,L (ALP-TRAP double staining): There are markedly fewer cells surrounding the newly formed bone in specimens recovered from the site of a conventional bone graft. (I, K) There are no blood vessels apparent and grafted autologous bone particles remain inside the fibrous membrane. Line-like narrow areas on the surface of the newly formed bone were immunopositive for ALP, albeit more weakly than the signals observed at the site of the autogenous bone graft with CAPCs. (J, L) TPAP-positive cells are rarely seen. *: newly formed bone, g: residual grafted autologous bone particles.

with CAPCs was generally satisfactory, and the predictability of alveolar bone augmentation was high even in large recipient sites. Nine maxillary SL sites had a sinus floor thickness of ≤2 mm, but use of CAPCs resulted in alveolar ridge augmentation with satisfactory morphology and long-term stable bone volume in these advanced cases of atrophy. No adverse events attributable to the use of CAPCs were found. One case with a background of chronic sinusitis showed progressive alveolar resorption after the sinus lift procedure. One site of partial exposure of the titanium-mesh and one site of partial fibrosis were observed on grafts. Graft materials containing more than 50% of the PRP glue were used in some of participants in this clinical study, and it was found that using CAPCs was beneficial for the satisfactory formation and long-term maintenance of bone in these participants. In other words, use of CAPCs can reduce the amount of autogenous bone that needs harvesting.

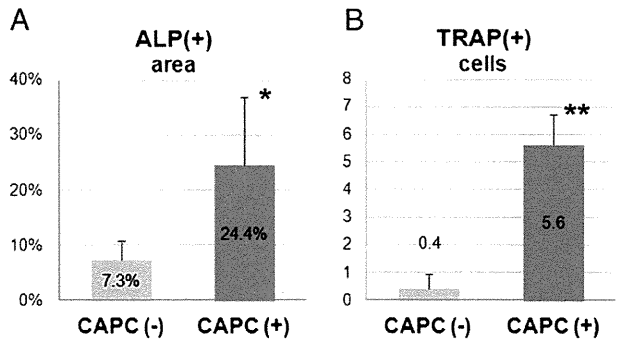

Fig. 3. Histomorphometric analysis of alkaline phosphatase (ALP) and the tartrate-resistant acid phosphatase activity (TRAP) of regenerated bone tissue. A: Comparative study by percentage of ALP-positive area between CAPC(+) bone grafts (n=4, 18–56 years, 44.5 years on average) and CAPC(−) bone grafts (n=4, 28–50 years, 39.0 years on average). B: Comparative study by the number of TRAP-positive cells per square between CAPC(+) bone grafts (n=5, 55–67 years, 55.6 years on average) and CAPC(−) bone graft (n=5, 28–64 years, 54.0 years on average). Analysis was done with a 870×650 μm² square view of histological sections. *: p<0.05; and **: P<0.001 (by t-test).

Recruitment of osteoblasts and osteoclasts to regenerating bone tissue

Fig. 2A–H shows the results of the histological analysis of biopsy specimens recovered from the recipient sites at 4 months after bone grafting with CAPCs. Spaces between the autogenous bone particles were filled with newly formed bone tissue. Layers of cells strongly immunopositive for ALP were present on the surface of the newly formed bone. Recruitment of TRAP-positive cells was confirmed for autogenous bone particles and the newly formed bone. In clear

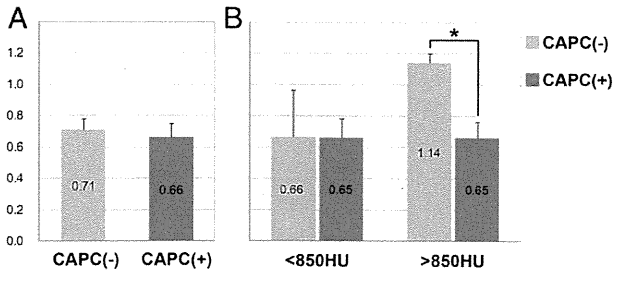

Fig. 4. Volumetric measurement of augmented bone at 3 M and 1Y after maxillary sinus lift.(A) Comparison of volumetric changes between cases of CAPC (+) bone grafting (n=4) and those of CAPC (−) bone grafting (n=3). There were no significant differences between the groups, and the volumes at 1Y were reduced to around 70% of those at 3 M regardless of use of CAPCs. (B) Comparison of volumetric changes in the low CT density area (<850 HU) and high CT density area (>850 HU). Time-dependent volume reductions by approximately 35% were found in the low CT density area, regardless of the use of CAPCs (<850HU: left in B). In the high CT density area, similar time-dependent reductions were found only for CAPC (+) bone grafts, while time-dependent volume reductions were absent at the sites of CAPC (−) bone grafts (>850HU: right in B). HU: Hounsfield units, *: p<0.05 (by t-test).

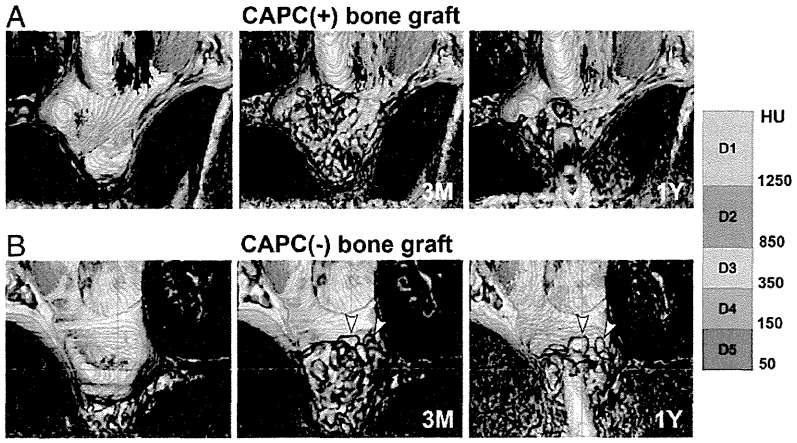

Fig. 5. 3D-CT images of the maxillary sinus constructed from DICOM data before surgery and at 3 months (3 M) and 1 year (1Y) after CAPC(+) bone graft (n = 4, 55–59 years, 58.0 years on average) or conventional CAPC(−) bone grafting (n = 3, age 35–64 years, 49.7 years on average). Color mapping of the images according to bone density as determined by Hounsfield units (HU) for CT data was applied to evaluate the quality of augmented bone. In the graft material at 3 M, many areas are depicted in light blue (D1) and blue (D2), indicative of autogenous cortical bone particles (A and B). (A) The formation of cortical bone layers with smooth surfaces is apparent on the upper surface of the augmented bone at 1Y after the CAPC (+) bone graft. (B) On the other hand, images of the site of the CAPC (−) bone graft reveals many D1 and D2 areas still remain at 1Y. Also, the same grafted cortical bone particles on the upper side of augmented bone at 3 M are exposed at 1Y after the graft (arrow heads in B).

contrast to these findings, in the biopsy specimens recovered 4 months after conventional bone grafting, markedly few cells were found around the newly formed bone, and ALP-positive signals, albeit weak, were found exclusively on the surface of the bone (Fig. 2I–L). Also, recruitment of TRAP-positive cells was negligible. Histomorphometric data revealed an increase in the ALP-positive area as well as the number of TRAP-positive cells with statistical significance (Fig. 3). These results indicate that the recruitment of both osteoblasts and osteoclasts to the regenerating bone tissue is markedly activated at the site of autogenous bone grafting with CAPC, compared to that of conventional bone grafting.

CAPC-induced bone remodeling after autogenous bone grafting

The volume of newly reformed bone tissue at 1Y was compared to that at 3 M in the 4 cases of maxillary SL with autologous bone and CAPCs and in the 3 cases of maxillary SL with autologous bone only (Fig. 4). The net volume of augmented bone was obtained by subtracting the volume of the implant screw from the volume calculated from the corresponding reconstructed 3D-CT image. Change in the mean net volume of augmented bone between the two time points was similar regardless of whether CAPCs were used (Fig. 4A). When compared after categorizing the area of augmented bone according to CT density, the mean volume was 35% lower at 1Y than at 3 M in the area with a CT density <850 HU, regardless of whether CAPCs were used or not (Fig. 4B, left). On the other hand, in the high density area (CT density >850), marked time-dependent decreases were found only after bone grafting with CAPCs, while no decrease were found in conventional bone grafting with statistical significance (Fig. 4B, right). Color-coded reconstructed 3D-CT images supported these findings (Fig. 5). The D2 and D1 areas (CT density >850), depicted in blue and light blue, in the image taken at 3 M were

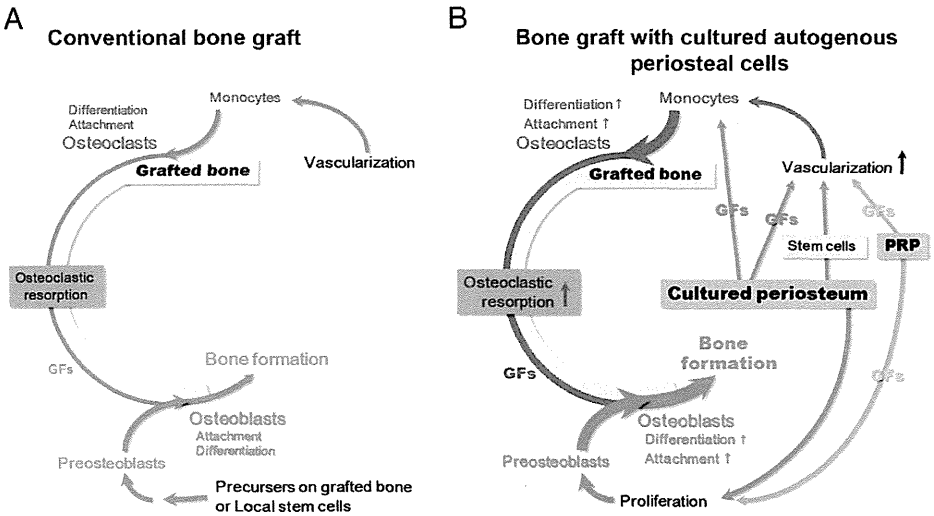

Fig. 6. Illustration of hypotheses for bone formation and resorption after (A) conventional bone grafting and (B) after bone grafting with CAPCs. (A) Bone tissue regeneration may rely on proliferation of a small population of osteogenic lineage cells after conventional bone grafting. The osteogenic and angiogenic cells are not active in the alveolar ridge, as it is surrounded by soft tissues, and therefore, recruitment and differentiation of osteoblasts and osteoclasts will be limited. (B) Grafted CAPCs may serve as a source of stem cells capable of giving rise to osteogenic progenitors and other cell types such as those necessary for angiogenesis, as well as serve as growth factor producers. Consequently, CAPCs play a comprehensive role in effectively promoting angiogenesis, and recruitment and differentiation of bone-resorbing cells. Grafted CAPCs will accelerate regeneration of functional bone with metabolic activity by supplying necessary cells and growth factors that activate both bone formation and bone resorption.

thought to correspond to cortical bone particles of mandibular origin contained in the graft material. These high CT density areas were almost absent in the 3D-CT images taken at 1Y after autogenous bone grafting with CAPCs, but a smooth surface area with high CT density areas with D1 and D2 levels was found on the surface of the augmented bone. At 1Y after conventional autogenous bone grafting, similar absorption of the augmented bone was observed, but cortical bone particles remained and were exposed at the surface of the augmented bone.

Discussion

In this study, as part of our ongoing clinical research into CAPC use in bone augmentation prior to the placement of dental implants, we investigated the effects of CAPCs on bone regeneration in 25 patients (33 sites), and satisfactory bone regeneration was found in most cases. Augmentation that is difficult to achieve by conventional autogenous bone grafting, such as that to build bone in both the directions of height and width in the alveolar ridge or to conduct a SL of ≥15 mm in patients with a less than 2-mm-thick maxillary sinus floor, became feasible through the application of CAPCs, regardless of age and sex of the patients. Results of histological and 3D-CT analyses suggested that grafted CAPCs effectively recruited osteoblasts and osteoclasts, thereby simultaneously promoting bone formation and remodeling.

Cell therapy for alveolar bone regeneration has been well studied. Animal studies have demonstrated the efficacy of mesenchymal stromal cells derived from various tissues [20–22], dental pulp cells [23], periodontal ligament [13], and periosteal cells [5,6,8–10,24] in bone regeneration. The possible roles these cells play in bone regeneration at the graft site are giving rise to osteoblasts and the constituent cells of blood vessels, and releasing growth factors to trigger paracrine or autocrine signaling, thereby inducing cell and tissue differentiation [25]. The purpose of cell therapy is to achieve rapid and high-quality bone regeneration in a wide area, which is impossible by autogenous bone grafting and the use of bone graft substitutes and growth factors.

Despite the extensive research undertaken using animal models, only a limited number of clinical studies have examined cell-based regenerative therapy, and further, the efficacy is not uniformly conclusive [7,26–32]. Variability in cell therapy efficacy may be explained by heterogeneity in the grafted cell populations, poor regenerative potential of human tissues, and biological influence from the scaffolding materials used. Also, the biological properties of regenerated bone tissue induced by cell grafting may not be appropriately depicted in clinical studies, because they tend to rely on image analysis such as examining X-ray absorption rates from CT images. In the present study, we performed morphometric and quantitative analysis of newly formed bone based on histological and high-resolution 3D-CT imaging findings, and successfully depicted the functional status of the regenerated bone. Histomorphometric and histological results indicated the possibility that CAPC grafting promoted active new bone formation and bone resorption by recruiting cells immunopositive for ALP activity and TRAP-positive cells, respectively. The findings of 3D-CT image analysis consistently suggested that CAPC grafting enhanced the resorption of the cortical bone particles grafted (Figs. 4 and 5). Also, similar to the conventional procedure, autogenous bone grafting with CAPCs maintained the volume and morphology of the augmented bone (Fig. 4 and 5). Taken together, these findings suggest the idea that the regenerated bone acquires its remodeling capability at an early stage after alveolar augmentation with CAPC grafting, and that the following osseointegration will secure the dental implant that is subsequently placed. The effects of CAPCs in regenerative bone therapy may be exerted via various biological mechanisms, as illustrated in Fig. 6. For instance, CAPCs may serve as the original cell population that gives rise to osteoblasts for bone matrix formation and to constituent cells of bone tissue such as vascular endothelial cells, as well as serve as a source of various growth factors, thereby recruiting and activating osteoclasts. The above hypothesis needs to be scientifically tested in the future.

Bone tissue engineering with CAPC grafting may enable regeneration of bone tissues with complex morphology in a wide area, and thus will expand indications for regenerative bone therapy. The autogenous bone content in the graft material is reduced to as low as 40% by use of CAPCs as of today. The less invasive approach releases the burden on patients, and also increases the volume of regenerative bone produced. However, autogenous bone particles serve as a secure scaffold for bone augmentation and thus are not replaceable. The ultimate goal is to establish procedures for CAPC culturing and grafting that enable regenerative bone therapy without harvesting bone. To achieve this goal, we must continue working on developing affordable and effective systems for regenerative bone therapy that also satisfy safety requirements.

Disclosure statement

We declare that there is no actual or potential conflict of interest including any financial, personal or other relationships with other people or organizations within 3 years of beginning the work submitted that could inappropriately bias this work.

Acknowledgments

The authors thank the staff of the Cell Processing Center of Niigata University Medical and Dental Hospital for continuous support in managing the cultivation of periosteal samples.

Funding source: The Japan Society for the Promotion of Science (Project Nos. 20592370 and 23592985).

References

[1] Gautschi OP, Frey SP, Zellweger R. Bone morphogenetic proteins in clinical applications. ANZ J Surg 2007;77:626–31.
[2] Wikesjö UM, Qahash M, Huang YH, Xiropaidis A, Polimeni G, Susin C. Bone morphogenetic proteins for periodontal and alveolar indications; biological observations - clinical implications. Orthod Craniofac Res 2009;12:263–70.
[3] Kodama N, Nagata M, Tabata Y, Ozeki M, Ninomiya T, Takagi R. A local bone anabolic effect of rhFGF2-impregnated gelatin hydrogel by promoting cell proliferation and coordinating osteoblastic differentiation. Bone 2009;44:699–707.
[4] Kitamura M, Akamatsu M, Machigashira M, Hara Y, Sakagami R, Hirofuji T, et al. FGF-2 stimulates periodontal regeneration: results of a multi-center randomized clinical trial. J Dent Res 2011;90:35–40.
[5] Mizuno H, Hata K, Kojima K, Bonassar LJ, Vacanti CA, Ueda M. A novel approach to regenerating periodontal tissue by grafting autologous cultured periosteum. J Tissue Eng 2006;12:1227–335.
[6] Mizuno D, Kagami H, Mizuno H, Mase J, Usami K, Ueda M. Bone regeneration of dental implant dehiscence defects using a cultured periosteum membrane. Clin Oral Implants Res 2008;19:289–94.
[7] Yamamiya K, Okuda K, Kawase T, Hata K, Wolff LF, Yoshie H. Tissue-engineered cultured periosteum used with platelet-rich plasma and hydroxyapatite in treating human osseous defects. J Periodontol 2008;79:811–8.
[8] Kawase T, Okuda K, Kogami H, Nakayama H, Nagata M, Nakata K, et al. Characterization of human cultured periosteal sheets expressing bone-forming potential: in vitro and in vivo animal studies. J Tissue Eng Regen Med 2009;3:218–29.
[9] Kawase T, Okuda K, Kogami H, Nakayama H, Nagata M, Yoshie H. Osteogenic activity of human periosteal sheets cultured on salmon collagen-coated ePTFE meshes. J Mater Sci Mater Med 2010;21:731–9.
[10] Kawase T, Tanaka T, Nishimoto T, Okuda K, Nagata M, Burns DM, et al. Improved adhesion of human cultured periosteal sheets to a porous poly (L-lactic acid) membrane scaffold without the aid of exogenous adhesion biomolecules. J Biomed Mater Res A 2011;98:100–13.
[11] Ito K, Yamada Y, Naiki T, Ueda M. Simultaneous implant placement and bone regeneration around dental implants using tissue-engineered bone with fibrin glue, mesenchymal stem cells and platelet-rich plasma. Clin Oral Implants Res 2006;17:579–86.
[12] Ueda M, Yamada Y, Kagami H, Hibi H. Injectable bone applied for ridge augmentation and dental implant placement: human progress study. Implant Dent 2008;17:82–90.
[13] Tsumanuma Y, Iwata T, Washio K, Yoshida T, Yamada A, Takagi R, et al. Comparison of different tissue-derived stem cell sheets for periodontal regeneration in a canine 1-wall defect model. Biomaterials 2011;32:5819–25.

[14] Zhang X, Xie C, Lin AS, Ito H, Awad H, Lieberman JR, et al. Periosteal progenitor cell fate in segmental cortical bone graft transplantations: implications for functional tissue engineering. J Bone Miner Res 2005;20:2124–37.
[15] Intini G. The use of platelet-rich plasma in bone reconstruction therapy. Biomaterials 2009;30:4956–66.
[16] Messora MR, Nagata MJ, Dornelles RC, Bomfim SR, Furlaneto FA, de Melo LG, et al. Bone healing in critical-size defects treated with platelet-rich plasma activated by two different methods. A histologic and histometric study in rat calvaria. J Periodontal Res 2008;43:723–9.
[17] Misch CE. Bone density: a key determinant for treatment planning. In: Misch CE, editor. Contemporary Implant Dentistry. third ed. St. Louis: Mosby; 2008. p. 130–46.
[18] Amizuka N, Shimomura J, Li M, Seki Y, Oda K, Henderson JE, et al. Defective bone remodelling in osteoprotegerin-deficient mice. J Electron Microsc (Tokyo) 2003;52:503–13.
[19] Oda K, Amaya Y, Fukushi-Irié M, Kinameri Y, Ohsuye K, Kubota I, et al. A general method for rapid purification of soluble versions of glycosylphosphatidylinositol-anchored proteins expressed in insect cells: an application for human tissue-nonspecific alkaline phosphatase. J Biochem (Tokyo) 1999;126:694–9.
[20] Yamada Y, Ueda M, Naiki T, Takahashi M, Hata K, Nagasaka T. Autogenous injectable bone for regeneration with mesenchymal stem cells and platelet-rich plasma: tissue-engineered bone regeneration. J Tissue Eng 2004;10:955–64.
[21] Tobita M, Uysal AC, Ogawa R, Hyakusoku H, Mizuno H. Periodontal tissue regeneration with adipose-derived stem cells. Tissue Eng Part A 2008;14:945–53.
[22] Wang L, Shen H, Zheng W, Tang L, Yang Z, Gao Y, et al. Characterization of stem cells from alveolar periodontal ligament. Tissue Eng Part A 2011;17:1015–26.
[23] Yamada Y, Nakamura S, Ito K, Sugito T, Yoshimi R, Nagasaka T, et al. A feasibility of useful cell-based therapy by bone regeneration with deciduous tooth stem cells, dental pulp stem cells, or bone-marrow-derived mesenchymal stem cells for clinical study using tissue engineering technology. Tissue Eng Part A 2010;16:1891–900.
[24] Zhu SJ, Choi BH, Huh JY, Jung JH, Kim BY, Lee SH. A comparative qualitative histological analysis of tissue-engineered bone using bone marrow mesenchymal stem cells, alveolar bone cells, and periosteal cells. Oral Surg Oral Med Oral Pathol Oral Radiol Endod 2006;101:164–9.
[25] Rios HF, Lin Z, Oh B, Park CH, Giannobile WV. Cell- and gene-based therapeutic strategies for periodontal regenerative medicine. J Periodontol 2011;82:1223–37.
[26] Schimming R, Schmelzeisen R. Tissue-engineered bone for maxillary sinus augmentation. J Oral Maxillofac Surg 2004;62:724–9.
[27] Springer IN, Nocini PF, Schlegel KA, De Santis D, Park J, Warnke PH, et al. Two techniques for the preparation of cell-scaffold constructs suitable for sinus augmentation: steps into clinical application. J Tissue Eng 2006;12:2649–56.
[28] Yamada Y, Nakamura S, Ito K, Kohgo T, Hibi H, Nagasaka T, et al. Injectable tissue-engineered bone using autogenous bone marrow-derived stromal cells for maxillary sinus augmentation: clinical application report from a 2-6-year follow-up. Tissue Eng Part A 2008;14:1699–707.
[29] Beaumont C, Schmidt RJ, Tatakis DN, Zafiropoulos GG. Use of engineered bone for sinus augmentation. J Periodontol 2008;79:541–8.
[30] Okuda K, Yamamiya K, Kawase T, Mizuno H, Ueda M, Yoshie H. Treatment of human infrabony periodontal defects by grafting human cultured periosteum sheets combined with platelet-rich plasma and porous hydroxyapatite granules: case series. J Int Acad Periodontol 2009;11:206–13.
[31] Voss P, Sauerbier S, Wiedmann-Al-Ahmad M, Zizelmann C, Stricker A, Schmelzeisen R, et al. Bone regeneration in sinus lifts: comparing tissue-engineered bone and iliac bone. Br J Oral Maxillofac Surg 2010;48:121–6.
[32] Park JB. Use of cell-based approaches in maxillary sinus augmentation procedures. J Craniofac Surg 2010;21:557–60.

Respiratory Physiology & Neurobiology 180 (2012) 112–118

Contents lists available at SciVerse ScienceDirect

Respiratory Physiology & Neurobiology

journal homepage: www.elsevier.com/locate/resphysiol

L-carbocisteine inhibits respiratory syncytial virus infection in human tracheal epithelial cells

Masanori Asada[a], Motoki Yoshida[a], Yukimasa Hatachi[b], Takahiko Sasaki[c], Hiroyasu Yasuda[d], Xue Deng[d], Hidekazu Nishimura[e], Hiroshi Kubo[f], Ryoichi Nagatomi[g], Mutsuo Yamaya[f,*]

[a] Department of Infectious Disease, Sendai City Hospital, Sendai, Japan
[b] Department of Respiratory Medicine, Graduate School of Medicine, Kyoto University, Kyoto, Japan
[c] Department of Respiratory Medicine, Tohoku University School of Medicine, Sendai, Japan
[d] Department of Innovation of New Biomedical Engineering Center, Tohoku University School of Medicine, Sendai, Japan
[e] Virus Research Center, Clinical Research Division, Sendai National Hospital, Sendai, Japan
[f] Department of Advanced Preventive Medicine for Infectious Disease, Tohoku University Graduate School of Medicine, 2-1 Seiryo-machi, Aoba-ku, Sendai 980-8575, Japan
[g] Medicine and Science in Sports and Exercise, Tohoku University Graduate School of Medicine, Sendai, Japan

ARTICLE INFO

Article history:
Accepted 27 October 2011

Keywords:
Bronchial asthma
Carbocisteine
COPD
ICAM-1
Respiratory syncytial virus

ABSTRACT

To examine the effects of L-carbocisteine on airway infection with respiratory syncytial (RS) virus, human tracheal epithelial cells were pretreated with L-carbocisteine and infected with RS virus. Viral titer, virus RNA, and pro-inflammatory cytokine secretion, including interleukin (IL)-1 and IL-6, increased with time after infection. L-carbocisteine reduced the viral titer in the supernatant fluids, the amount of RS virus RNA, RS virus infection susceptibility, and the concentration of pro-inflammatory cytokines induced by virus infection. L-carbocisteine reduced the expression of intercellular adhesion molecule (ICAM)-1, an RS virus receptor, on the cells. However, L-carbocisteine had no effects on the expression of heparan sulfate, a glycosaminoglycan that binds to the RS virus attachment protein, or on the amount of intracellular activated-RhoA, isoform A of the Ras-homologous family, that binds to the RS virus fusion protein. These findings suggest that L-carbocisteine may inhibit RS virus infection by reducing the expression of ICAM-1. It may also modulate airway inflammation during RS virus infection.

1. Introduction

Respiratory syncytial (RS) virus is one of the important pathogens responsible for common colds (Hayden and Gwaltney, 1988) and is the major cause of viral lower respiratory tract disease in infants and young children (Collins and Crowe, 2006). Relationships have been reported between wheezing-associated respiratory illness and RS virus outbreaks in children (Henderson et al., 1979), and between RS virus infection and exacerbation of chronic obstructive pulmonary disease (COPD) (Guidry et al., 1991).

The RS virus attachment protein (G protein), which binds to the receptor for RS virus (Collins and Crowe, 2006), interacts with glycosaminoglycans (GAGs) containing the disaccharides heparan sulfate and chondroitin sulfate B (Feldman et al., 1999; Hallak et al., 2000). The RS virus F glycoprotein, which also binds to the receptor for RS virus (Collins and Crowe, 2006), can interact with activated intracellular protein RhoA (Budge et al., 2003; Pastey et al., 1993), isoform A of a small guanosine triphosphatase (GTPase) of the Ras super family (Rho, Ras-homologous) (Takai et al., 2001). ICAM-1 facilitates RS virus entry and the infection of human epithelial cells by binding to the RS virus fusion protein (F protein) (Behera et al., 2001).

The F protein promotes the fusion of the viral and cellular membranes and the subsequent transfer of the viral genome material into the cell (Collins and Crowe, 2006). The F protein also promotes syncytia formation of the infected cells (Collins and Crowe, 2006). Pastey et al. (2000) demonstrated the inhibitory effects of a RhoA-derived peptide on syncytium formation induced by RS virus. We previously reported that macrolide antibiotics inhibit RS virus infection by reducing the levels of activated RhoA and inhibiting the subsequent activation of Rho kinase in human airway epithelial cells (Asada et al., 2009). Soluble ICAM-1 also inhibits epithelial cell infection by RS virus (Behera et al., 2001). As we previously demonstrated (Yasuda et al., 2006b), L-carbocisteine reduces ICAM-1 expression in human tracheal epithelial cells and inhibits infection with rhinovirus, a major cause of common colds. However, the effects of L-carbocisteine on RS virus infection remain unclear.

Exacerbation of bronchial asthma and COPD is associated with a variety of mediators, including interleukin (IL)-6 and IL-8, the

* Corresponding author. Tel.: +81 22 717 7184; fax: +81 22 717 7576.
E-mail address: myamaya@med.tohoku.ac.jp (M. Yamaya).

1569-9048/$ – see front matter © 2011 Elsevier B.V. All rights reserved.
doi:10.1016/j.resp.2011.10.017

production and secretion of which are stimulated by RS virus in airway epithelial cells (Noah and Becker, 1993; Tripp et al., 2005). Although L-carbocisteine has been shown to reduce the production of pro-inflammatory cytokines after rhinovirus infection (Yasuda et al., 2006b), the inhibitory effects of L-carbocisteine on the induction of pro-inflammatory cytokines by RS virus infection are undetermined.

Therefore, we examined the inhibitory effects of L-carbocisteine on RS virus infection and the production of cytokines. We also investigated the mechanisms responsible for inhibition of RS virus infection.

2. Methods

2.1. Human tracheal epithelial cell culture

The isolation and culture of human tracheal surface epithelial cells were performed as previously described (Asada et al., 2009). The cells were plated at 5×10^5 viable cells/ml in round bottom plastic tubes (16 mm diameter and 125 mm length, Becton Dickinson and Co.). The cells were immersed in 1 ml of Dulbecco's Modified Eagle's Medium (DMEM)/Ham's F-12 medium (50/50, vol/vol) (GIBCO-BRL Life Technologies, Palo Alto, CA) containing 2% ultroser G (BioSepra, Cergy-Saint-Christophe, France) and cultured at 37 °C in 5% CO_2–95% air in an incubator. This study was approved by the Tohoku University Ethics Committee.

2.2. Culture of human epithelial Hep-2 cells

Human epithelial Hep-2 cells were cultured in flasks (25 cm^2 surface area; Becton Dickinson) in minimum essential medium (MEM) containing 5% calf serum supplemented with antibiotics and glucose, as previously described (Asada et al., 2009; Numazaki et al., 1987). The cells were then plated in plastic dishes (96-well plate, Becton Dickinson) or in plastic tubes.

2.3. Viral stocks

Respiratory syncytial (RS) virus was isolated in our laboratory from a patient with a common cold (Numazaki et al., 1987), and we found that the RS virus used in this study was type A (Asada et al., 2009). RS virus stocks were generated by infecting Hep-2 cells with RS virus in plastic tubes, as previously described (Asada et al., 2009).

2.4. Detection and titration of viruses

The detection and titration of RS viruses in the supernatant fluids of human tracheal epithelial cells were performed using the endpoint method (Condit, 2006) by infecting replicate wells of confluent Hep-2 cells in plastic 96-well dishes with serial 10-fold dilutions of virus-containing supernatant fluids, as previously described (Asada et al., 2009). To measure RS virus titers in the supernatant fluids of human tracheal epithelial cells, the fluids were added to Hep-2 cells in the wells of plastic dishes and the presence of the large syncytium, which shows typical cytopathic effects (CPE) of RS virus (Condit, 2006), was observed for 7 days. The dilution of virus-containing supernatant fluids that showed typical CPE of RS virus in greater than 50% of replicate wells and the dilution that showed CPE in less than 50% of replicate wells were estimated. Based on these data, the 50% tissue culture infective dose ($TCID_{50}$) was calculated using the methods as previously described (Condit, 2006). Because the cells were cultured in tubes with 1 ml of medium, the viral titers in the supernatant fluids were expressed as $TCID_{50}$ units/ml (Asada et al., 2009; Condit, 2006).

2.5. Viral infection of human tracheal epithelial cells

Infection of human tracheal epithelial cells by RS virus was performed using previously described methods (Asada et al., 2009). A stock solution of RS virus (100 μl per tube, 1.0×10^4 $TCID_{50}$ units/ml) was added to the cells in the tubes ($2.1 \pm 0.3 \times 10^6$ cells/tube, $n = 7$) and incubated for 1 h at 33 °C in 5% CO_2–95% air. The multiplicity of infection (moi) was 0.5×10^{-3} $TCID_{50}$ units/cell (Asada et al., 2009). The cells were then fed with 1 ml of fresh DF-12 medium containing 2% USG and cultured by rolling at 33 °C in an incubator (HDR-6-T, Hirasawa, Tokyo, Japan), as previously described (Asada et al., 2009; Numazaki et al., 1987).

2.6. Treatment of cells with L-carbocisteine

Human tracheal epithelial cells were treated with 10 μM L-carbocisteine from 3 days prior to RS virus infection until the end of the experiments following RS virus infection (Asada et al., 2009; Yasuda et al., 2006b) unless other concentrations or treatment periods are described. This concentration of L-carbocisteine (10 μM) was chosen because the maximum concentration of L-carbocisteine in the serum was 78 μM at 2 h after the oral ingestion of 1500 mg of L-carbocisteine, and mean serum concentration was 4.9 μM at 10 h after ingestion (De Schutter et al., 1988).

To study the relationship between pre-incubation time and the potency of the inhibitory effects, we examined the effects of pre-treatment time on viral titer in supernatant fluids. Human tracheal epithelial cells were pretreated with L-carbocisteine for periods ranging from 0 to 72 h. In preliminary experiments, we found that consistent inhibitory effects were obtained when the cells were pretreated with L-carbocisteine for 72 h. Therefore, cells were pre-treated with L-carbocisteine for 72 h (3 days) in this study.

We also studied the relationship between the concentration of L-carbocisteine and the potency of the inhibitory effects.

L-carbocisteine was dissolved in 0.1 N of NaOH and then neutralized with 0.1 N of HCl in this study, according to the manufacturer's instructions.

2.7. Collection of supernatant fluids for viral titer measurements

Supernatant fluids (1 ml) were collected at 2 h, 1 day (24 h), 3 days or 5 days after RS virus infection, as previously described (Asada et al., 2009).

To measure RS virus release during the first 24 h, we used 2 separate cultures from the same trachea. We collected the supernatant fluids at either 2 h or 24 h after RS virus infection. We also collected supernatant fluids at 3 days (72 h) and 5 days (120 h). At 1 day (24 h) and 3 days (72 h) after infection, supernatant fluids were collected, fresh medium was replaced, and the cell culture was continued.

2.8. The effects of L-carbocisteine on susceptibility to RS virus infection

The effects of L-carbocisteine on susceptibility to RS virus infection were examined as previously described (Asada et al., 2009). The human tracheal epithelial cells were treated with 10 μM L-carbocisteine from 3 days prior to RS virus infection until just after infection. The cells were then exposed to serial 10-fold dilutions of RS virus for 1 h at 33 °C. The presence of RS virus in the supernatant fluids collected 3–5 days after infection was determined using the methods described above (Section 2.4).

2.9. Quantification of RS virus RNA

RS virus RNA and rRNA expressions were quantified in human tracheal epithelial cells following RS virus infection. Real-time

quantitative RT-PCR using the TaqMan technique (Roche Molecular Diagnostic Systems) was performed on RNA extracted from the RS virus-infected cells as previously described (Asada et al., 2009; Yamaya et al., 2011).

In the first step, cDNA was generated from RS virus RNA with the QuantiTect Reverse Transcription Kit (Qiagen) using the RS virus reverse primer (5′-TGTCCCTCAGCTTTTTGATATCATC-3′).

In the second step, real-time PCR was performed using cDNA generated from RS virus RNA with a TaqMan® Gene Expression Master Mix (Asada et al., 2009; Yamaya et al., 2011). A sample of the cDNA produced in the first step was mixed with TaqMan Gene Expression Master Mix, a forward primer (5′-TGGTGTAGTTGGAGTGCTAGAGAGAGTT-3′), a reverse primer (5′-TGTCCCTCAGCTTTTTGATATCATC-3′), and a Taqman probe [5′-(FAM) CTAAACAATCAGCATGTGTTGCCATGAGCA (TAMRA)-3′] for the RS virus, and RNAase-free water.

To quantify the rRNA, the conversion of rRNA to cDNA and real-time PCR were performed using the same two-step process described above. A forward primer (5′-GCACTTCTGTTTCCCAGGAGC-3′), a reverse primer (5′-CGGACACCCAAAGTAGTCGGT-3′), and Taqman probe (5′-[FAM] CCTTTAACCGTTATCCGCCA [TAMRA]-3′) were designed for rRNA.

The minimum PCR cycle required to detect the fluorescent signal was defined as the cycle threshold (C_T) of the RS virus RNA and rRNA, and quantitative data were obtained as previously described (Asada et al., 2009; Yamaya et al., 2011).

2.10. Measurement of ICAM-1 expression

The ICAM-1 mRNA was examined by two-step real-time RT-PCR analysis using the same methods described for the RS virus RNA. A forward primer (5′-GCACTTCTGTTTCCCAGGAGC-3′), a reverse primer (5′-CGGACACCCAAAGTAG TCGGT-3′), and a Taqman probe (5′-[FAM] CCTTTAACCGTTATCCGCCA [TAMRA]-3′) were designed for ICAM-1. The expression of ICAM-1 mRNA was normalized to the constitutive expression of rRNA. The concentration of sICAM-1 in the supernatant fluids was measured with an enzyme immunoassay (EIA) (Yamaya et al., 2011).

2.11. Measurement of RhoA activation

RhoA activation was assessed using a previously described method (Asada et al., 2009; Chikumi et al., 2002; Kadowaki et al., 2004; Yamaguchi et al., 2001). A GTP-bound form of RhoA (RhoA-GTP) associated with a GST-Rho-binding domain (GST-RBD) was reported to show RhoA activation (Chikumi et al., 2002; Kadowaki et al., 2004; Yamaguchi et al., 2001). RhoA-GTP levels were quantified by western blot analysis. In brief, human tracheal epithelial cells were pretreated with 10 μM L-carbocisteine for 3 days. After stimulation with lysophosphatidic acid (LPA) (1 μM for 5 min) (Mills and Moolenaar, 2003), the cells were lysed and incubated with a glutathione S-transferase (GST) fusion protein that included the Rho-binding domain (RBD) of rhotekin. RhoA-GTP associated with GST-RBD was quantified by western blot analysis using a monoclonal antibody against RhoA (26C4; Santa Cruz Biotechnology, Santa Cruz, CA). The western blot membranes were subsequently incubated with suitable horseradish peroxidase-coupled secondary antibodies. The bands were visualized using an ECL chemiluminescence kit (Amersham Biosciences, Piscataway, NJ) and CCD camera. The bands were quantified by densitometric scanning using the ImageJ imaging processing program (http://rsb.info.nih.gov/ij/index.html) (Hegab et al., 2008).

2.12. Measurement of heparan sulfate

Expression of heparan sulfate, a glycosaminoglycan (GAG) that binds to the RS virus G protein, was measured by flow cytometry (Dechecchi et al., 2001). Cultured human tracheal epithelial cells in 6-well plates were rinsed with PBS without magnesium or calcium and treated with 1 ml of a nonenzymatic EDTA-containing cell dissociation solution (Cell Dissociation Solution Non-enzymatic 1×®, Sigma, St. Louis, MO, USA) for 10 min (Wu et al., 1997). Detached cells were then collected, and cells (2×10^7/ml) in 0.5% casein-PBS were incubated with 20 mg/ml of F58-10E4 immunoglobulin M monoclonal antibody (Seikagaku Co., Tokyo, Japan) directed against heparan sulfate for 2 h at 4 °C, followed by incubation with 50 mg/ml fluorescein-conjugated goat anti-mouse immunoglobulin M antibody (Sigma) for 30 min at 4 °C in PBS. The cells were fixed with 4% formaldehyde in PBS and analyzed using a FACScan flow cytometer (Becton Dickinson).

Furthermore, the concentration of heparan sulfate in the supernatant fluids of human tracheal epithelial cells was measured by specific enzyme-linked immunosorbent assays (ELISAs) using the Heparan Sulfate ELISA Kit (Seikagaku Co., Tokyo, Japan) (Raats et al., 1997).

2.13. Measurement of cytokine production

We measured the concentration of IL-1β, IL-6 and IL-8 in the supernatant fluids of human tracheal epithelial cells by ELISA, as previously described (Asada et al., 2009). We measured the secretion of cytokines before infection and at 3 days after infection with RS virus, which was when the maximum cytokine secretion was observed.

2.14. Statistical analysis

The results are expressed as the mean ± SEM. Statistical analysis was performed using one-way analysis of variance (ANOVA). Subsequent post hoc analysis was performed using Bonferroni's method. For all analyses, values of $p < 0.05$ were assumed to be significant. In the experiments using cultures of human tracheal epithelial cells, n refers to the number of donors (tracheae) from which cultured epithelial cells were used.

3. Results

3.1. The effects of L-carbocisteine on RS virus infection of human tracheal epithelial cells

Exposure of confluent human tracheal epithelial cell monolayers to RS virus (0.5×10^{-3} $TCID_{50}$ units/cell) consistently led to infection. The supernatant fluids from human tracheal epithelial cells 2 h after RS virus infection did not contain a significant amount of viruses. Hep-2 cells did not show any syncytia formation, which indicates the typical cytopathic effects (CPE) of RS virus, when the supernatant fluids were collected from human tracheal epithelial cells at 2 h after RS virus infection and added to the Hep-2 cells (data not shown). However, the supernatant fluids of human tracheal epithelial cells at 1 day (24 h) after RS virus infection contained a significant amount of viruses (Fig. 1A). The addition of supernatant fluids from human tracheal epithelial cells, which were collected at 1 day after infection, resulted in syncytia formation in the Hep-2 cells (data not shown). RS virus was detected in supernatant fluids at 1 day after infection, and the viral content progressively increased between 1 and 5 days after infection (Fig. 1A). RS virus infection of the cells was constant, and evidence of continuous viral production was obtained by demonstrating that each batch of supernatant fluid collected during the intervals from 0 to 1 day,

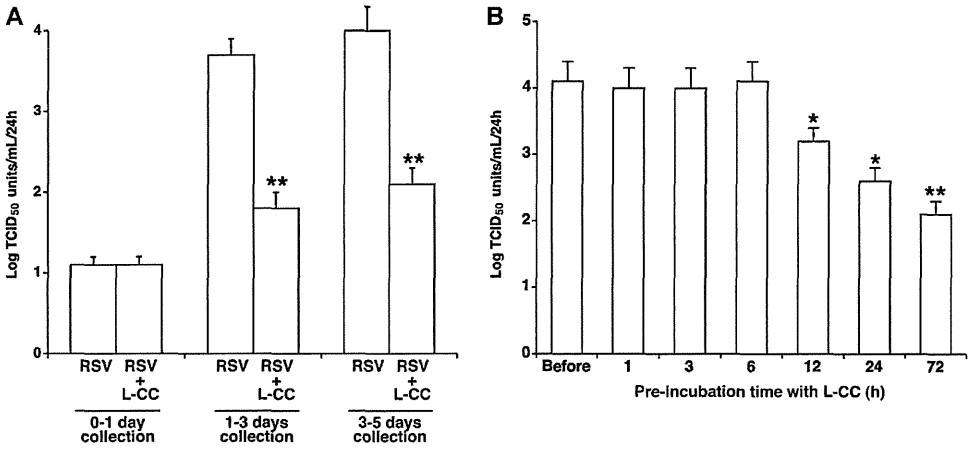

Fig. 1. (A) Time course of RS viral titers in the supernatant fluids of human tracheal epithelial cells after exposure to RS virus in the presence of L-carbocisteine (10 μM) (RSV + L-CC) or a vehicle (0.1% double-distilled water) (RSV). The rates of change in the RS virus concentration in the supernatant fluids are expressed as $TCID_{50}$ units/ml/24 h. The results are reported as the mean ± SEM of five different tracheae. Significant differences in comparison to viral infection alone (RSV) are indicated by asterisks (**$p < 0.01$). (B) Viral titers in the supernatant fluids collected during the intervals 3–5 days after infection from the cells pretreated with L-carbocisteine (L-CC) for periods ranging from 0 to 72 h. The viral titers in supernatant fluids are expressed as $TCID_{50}$ units/ml/24 h. The results are reported as the mean ± SEM of five different tracheae. Significant differences in comparison to viral infection alone (before) are indicated by asterisks (*$p < 0.05$ and **$p < 0.01$).

1 to 3 days and 3 to 5 days after infection contained significant levels of RS virus (Fig. 1A). The viral titers in the supernatant fluids increased significantly with time over the 5 days of observation ($p < 0.05$ in each case by ANOVA).

Treatment of the human tracheal epithelial cells with 10 μM L-carbocisteine significantly decreased the viral titers in the supernatant fluids collected during the intervals 1–3 days and 3–5 days after infection (Fig. 1A), while the viral titers in the supernatant fluids collected during the 0–1 day interval in the cells treated with L-carbocisteine did not differ from those in the cells treated with vehicle (0.1% double distilled water) (Fig. 1A).

In the cells pretreated with L-carbocisteine (10 μM), a significant reduction of the viral titer was observed when the cells were pre-incubated for 12 h or longer (Fig. 1B). The reduction in viral titer in the supernatant fluids depended on the pre-incubation time, and viral titers in the cells pretreated with L-carbocisteine for 72 h were lower than those in the cells pretreated for 24 h (Fig. 1B).

L-carbocisteine reduced the viral titer in the supernatant fluids in a dose-dependent manner, and the maximum effect was obtained at 100 μM (Fig. 2).

To determine whether or not L-carbocisteine-induced cytotoxic effects caused cell detachment of confluent cells in the culture vessels of the plastic tubes, cell numbers were counted after treatment with L-carbocisteine or vehicle. L-carbocisteine treatment (10 μM; 5 days) did not have any effect on the number of human tracheal epithelial cells (2.1×10^6 cells/tube in vehicle treatment vs. 2.0×10^6 cell/tube in L-carbocisteine treatment) ($p > 0.50$; $n = 3$). Cell viability, assessed by trypan blue exclusion (Yasuda et al., 2006b), was consistently >96% in the carbocisteine-treated culture. Furthermore, L-carbocisteine treatment did not alter the amount of lactate dehydrogenase (LDH) in the supernatant fluids of human tracheal epithelial cells. The amount of LDH in the supernatant fluids was 30 ± 2 IU/l after treatment with vehicle, and 31 ± 2 IU/l after L-carbocisteine treatment (10 μM; 5 days) ($p > 0.50$; $n = 3$).

3.2. The effect of L-carbocisteine on viral RNA by PCR

RNA extraction was performed at 72 h and 120 h after RS virus infection. RS viral RNA replication in the cells was consistently observed at 72 h and 120 h after infection (Fig. 3) and increased between 72 h and 120 h after infection (Fig. 3). L-carbocisteine (10 μM) decreased the amount of RS viral RNA present at 72 and 120 h after infection (Fig. 3).

3.3. The effect of L-carbocisteine on susceptibility to RS virus infection

Treatment of the human tracheal epithelial cells with L-carbocisteine (10 μM) decreased the susceptibility of the cells to infection by RS virus. The minimum dose of RS virus necessary to cause infection in the cells treated with L-carbocisteine (10 μM, 3 days) (3.3 ± 0.2 $TCID_{50}$ units/ml, $n = 5$, $p < 0.05$) was significantly higher than that for the cells treated with the vehicle alone (2.2 ± 0.2 $TCID_{50}$ units/ml, $n = 5$).

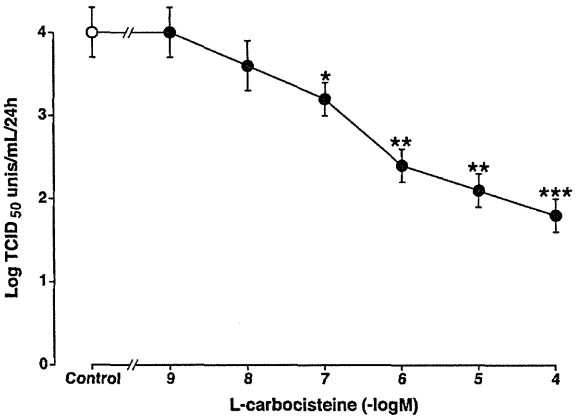

Fig. 2. A dose–response curve for the effect of L-carbocisteine on viral titer in the supernatant fluids collected during the intervals 3–5 days after infection. The human tracheal epithelial cells were treated with either L-carbocisteine or vehicle (control) from 3 days prior to RS virus infection until the end of the experimental period after RS virus infection. Viral titers in the supernatant fluids are expressed as $TCID_{50}$ units/ml/24 h. The results are reported as the mean ± SEM of five different tracheae. Significant differences from the vehicle alone (control) are indicated by asterisks (*$p < 0.05$, **$p < 0.01$ and ***$p < 0.001$).

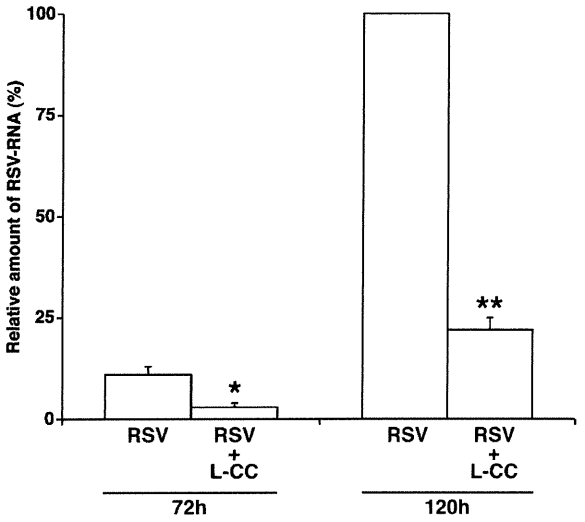

Fig. 3. Replication of RS virus RNA in human tracheal epithelial cells infected with RS virus in the presence of L-carbocisteine (10 μM; RSV+L-CC) or a vehicle (control; RSV). The results are expressed as a percentage of the maximal RS virus RNA expression measured on day 5 (120 h) in the vehicle-treated cells, and the results are reported as the mean ± SEM of five samples. Significant differences from the vehicle treatment (RSV) at each time point are indicated by asterisks (*$p < 0.05$ and **$p < 0.01$). The RS virus RNA level on day 5 (120 h) in the vehicle-treated cells was 0.14 ± 0.02 ($n = 5$) relative to the amount of rRNA.

3.4. The effect of L-carbocisteine on the ICAM-1 expression

L-carbocisteine (10 μM, 72 h) reduced the baseline mRNA expression of ICAM-1 by approximately 40% in comparison to human tracheal epithelial cells treated with the vehicle alone before RS virus infection (Fig. 4A). Furthermore, the concentrations of sICAM-1 in the supernatant fluids of the cells treated with L-carbocisteine (10 μM) were significantly lower than in the cells treated with the vehicle alone before the RS virus infection (Fig. 4B).

3.5. The effect of L-carbocisteine on RhoA activation

A GTP-bound form of RhoA (GTP-bound RhoA, RhoA-GTP) associated with a GST-Rho-binding domain (GST-RBD) was reported to show RhoA activation (Chikumi et al., 2002; Kadowaki et al., 2004; Yamaguchi et al., 2001). On a western blot, the band corresponding to RhoA-GTP was faintly visible in the baseline condition, and the density of the RhoA-GTP band was increased after cellular stimulation with lysophosphatidic acid (LPA, 1 μM for 5 min) (data not shown). The relative ratio of the band density of RhoA-GTP to that of total RhoA in the human tracheal epithelial cells stimulated with LPA was 0.87 ± 0.03 ($n = 5$). L-carbocisteine (10 μM) did not reduce the density of the RhoA-GTP bands (0.85 ± 0.03, $n = 5$, $p > 0.20$) in the cells stimulated with LPA.

3.6. The effect of L-carbocisteine on the expression of heparan sulfate

Primary cultures of human tracheal epithelial cells consistently expressed heparan sulfate, as detected by flow cytometry. Analyzed by flow cytometry, the fluorescence intensity of the cells treated with L-carbocisteine (10 μM) (17.8 ± 1.8, $n = 5$) did not differ from that of the cells treated with vehicle alone (19.2 ± 1.6, $n = 5$, $p > 0.20$) prior to the RS virus infection.

Likewise, a significant amount of heparan sulfate was observed in the supernatant fluids of the human tracheal epithelial cells. The concentrations of heparan sulfate in the supernatant fluids of the cells treated with L-carbocisteine (10 μM) did not differ from those of the cells treated with the vehicle alone before the RS virus infection. In ELISA assays, the absorbance intensity in the supernatant fluids of the cells treated with L-carbocisteine (4.8 ± 0.4, $n = 5$) did not differ from that of the cells treated with the vehicle alone (4.7 ± 0.4, $n = 5$, $p > 0.50$).

3.7. The effect of L-carbocisteine on cytokine production

The secretion of IL-1β, IL-6 and IL-8 all increased in the supernatant fluids of human tracheal epithelial cells after RS virus

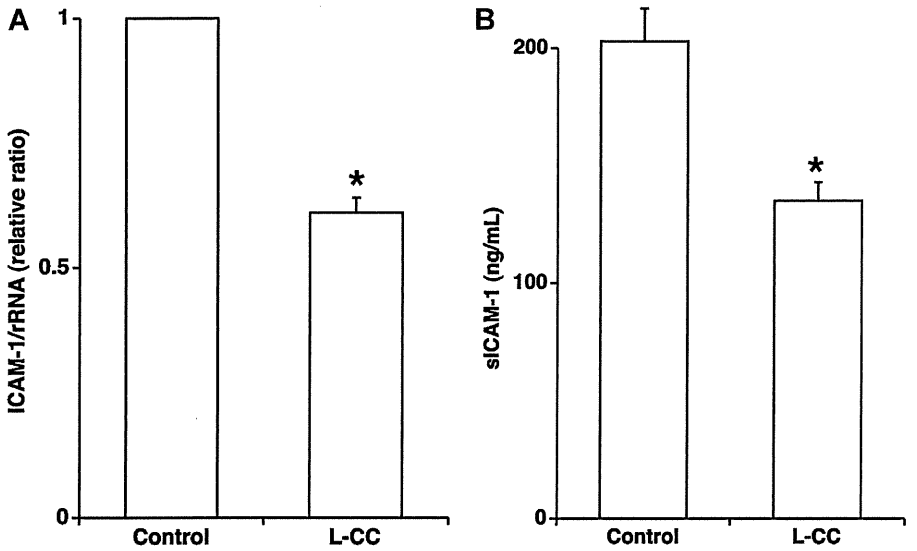

Fig. 4. (A) ICAM-1 mRNA expression in uninfected cells treated with L-carbocisteine (L-CC, 10 μM) or a vehicle (control), as detected by real-time quantitative RT-PCR. Human tracheal epithelial cells isolated from the same donors were treated with either L-carbocisteine or vehicle. ICAM-1 mRNA was normalized to the constitutive expression of ribosomal RNA (rRNA). The ICAM-1 mRNA expression in the cells treated with the vehicle (control) was set to 1.0. The results are reported as the mean ± SEM of five different tracheae. Significant differences from the control values are indicated by an asterisk (*$p < 0.05$). (B) The concentrations of sICAM-1 in the supernatant fluids from uninfected human tracheal epithelial cells treated with L-carbocisteine (L-CC, 10 μM) or a vehicle (control). The concentrations of sICAM-1 in the supernatant fluids are expressed as ng/ml. The results are expressed as the mean ± SEM of five different tracheae. Significant differences from the control values are indicated by an asterisk (*$p < 0.05$).

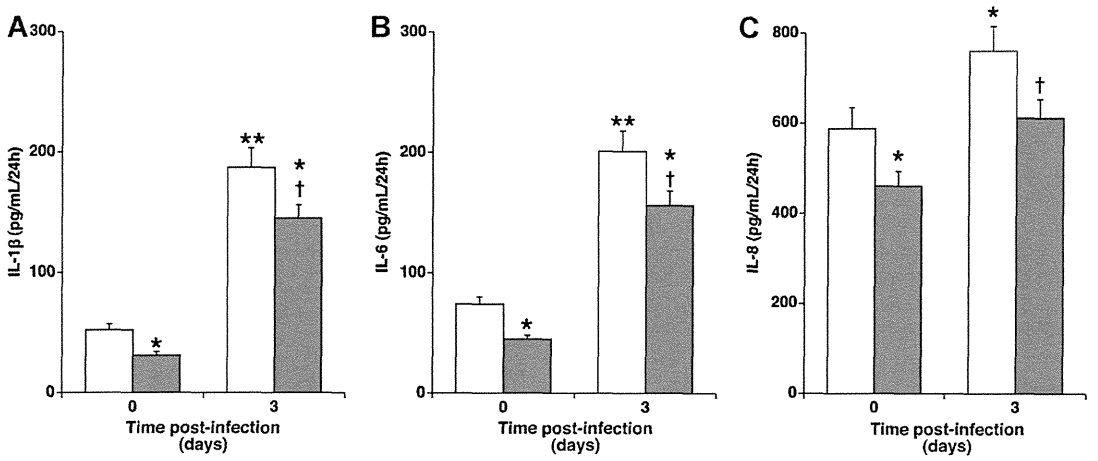

Fig. 5. The release of cytokines into the supernatant fluids of human tracheal epithelial cells prior to infection (time 0; for 24 h before infection) and the fluids collected during the intervals 1–3 days after RS virus infection in the presence of either L-carbocisteine (10 μM; gray bars) or vehicle (white bars). The rates of change in cytokine concentrations in the supernatant fluids are expressed as pg/ml/24 h. The results are reported as the mean ± SEM of five different tracheae. Significant differences from the values prior to RS virus infection in the presence of vehicle (white bars, time 0) are indicated by asterisks ($^{*}p < 0.05$ and $^{**}p < 0.01$). Significant differences from the values with RS virus plus vehicle 3 days after RS virus infection (white bars, time 3 days) are indicated by plus signs ($+p < 0.05$).

infection (Fig. 5), and the maximum secretion was observed 3 days after the infection (data from days 1 and 5 not shown). Treatment with L-carbocisteine (10 μM) reduced the concentrations of IL-1β, IL-6 and IL-8 produced 3 days after RS virus infection and the baseline concentrations of these cytokines before the RS virus infection (Fig. 5).

4. Discussion

In this study, we showed that RS virus titers in the supernatant fluids and the amount of RS virus RNA in the human tracheal epithelial cells increased with time. A mucolytic agent, L-carbocisteine, reduced the titers of RS virus in the supernatant fluids in a dose-dependent manner, in addition to reducing RS virus RNA replication and susceptibility to RS virus infection. L-carbocisteine inhibited the expression of ICAM-1, an RS virus receptor (Behera et al., 2001), but did not inhibit the activation of RhoA, which is associated with RS virus infection via binding to its F protein (Budge et al., 2003; Pastey et al., 1993). L-carbocisteine did not reduce the expression of heparan sulfate, a GAG that binds to the RS virus G protein (Feldman et al., 1999; Hallak et al., 2000). These findings suggest that L-carbocisteine may inhibit RS virus infection, partly through the reduced expression of ICAM-1, in human airway epithelial cells. L-carbocisteine may also modulate the airway inflammation that is induced by RS virus infection.

Hep-2 cells did not show any syncytia formation when the supernatant fluids were collected at 2 h after RS virus infection and added to the Hep-2 cells. In contrast, supernatant fluids collected at 1 day (24 h) after infection induced syncytia formation in Hep-2 cells, which demonstrates that the supernatant fluids of human tracheal epithelial cells collected 1 day after infection contained significant amounts of RS virus. These findings suggest that supernatant fluids collected at 1 day after infection contained significant amounts of RS virus, which was newly produced after infection.

RhoA, an isoform A of the Rho family (Takai et al., 2001), has various functions including stimulus-induced cell adhesion and motility, the enhancement of contractile responses, and cytokinesis (Narumiya, 1996). Furthermore, the activated form of RhoA moves to the cell membrane and is implicated in RS virus infection via binding to its F protein (Collins and Crowe, 2006; Pastey et al., 1993). Behera et al. (2001) demonstrated that RS virus colocalizes with ICAM-1 on the Hep-2 cell surface, and a neutralizing anti-ICAM-1 antibody inhibits RS virus infection. Incubation of the virus with soluble ICAM-1 inhibited RS virus infection of epithelial cells, and RS virus binds to ICAM-1, which can be inhibited by an antibody to the fusion F protein. The recombinant F protein can bind to soluble ICAM-1. These findings suggest that ICAM-1 facilitates RS virus entry and the infection of human epithelial cells by binding to the RS virus F protein (Behera et al., 2001). Iesato et al. (2008) reported that a long-acting anti-cholinergic agent, tiotropium, reduces RS virus replication partly through the inhibition of ICAM-1 expression in Hep-2 cells. Reduced expression of ICAM-1 in human tracheal epithelial cells, as observed in this study, is consistent with the findings of a previous report (Yasuda et al., 2006b). L-carbocisteine might inhibit RS virus infection, partly through the reduced expression of ICAM-1, in human airway epithelial cells in this study, whereas it might not inhibit the activation of RhoA.

Heparan sulfate and chondroitin sulfate also act as receptors for the RS virus (Collins and Crowe, 2006). We examined the effects of L-carbocisteine on the expression of heparan sulfate. However, L-carbocisteine did not reduce the expression of heparan sulfate in human tracheal epithelial cells, and the concentrations of heparan sulfate in the supernatant fluids from the cells treated with L-carbocisteine did not differ from those from cells treated with the vehicle alone.

In this study, RS virus infection increased the production of IL-1β, IL-6 and IL-8. L-carbocisteine reduced the production of IL-1β, IL-6 and IL-8 after RS virus infection. L-carbocisteine also reduced viral titers in the supernatant fluids. However, L-carbocisteine reduced the baseline production of these cytokines prior to RS virus infection. Reduced production of cytokines by L-carbocisteine in the absence of virus infection is consistent with the results in a previous report (Yasuda et al., 2006b). Therefore, these findings suggest that the reduced production of these cytokines in the cells treated with L-carbocisteine after RS virus infection might be caused by two mechanisms: the inhibitory effects of L-carbocisteine on RS virus infection and its effects on cytokine production.

A relationship has been reported between RS virus infection and development of exacerbations of COPD (Guidry et al., 1991). L-carbocisteine reduces the frequency of the common cold (Tatsumi and Fukuchi, 2007; Yasuda et al., 2006a) and the frequency of exacerbations (Tatsumi and Fukuchi, 2007; Yasuda et al., 2006a; Zheng et al., 2008) in COPD patients. Although another mucolytic

agent, N-acetylcysteine, has no significant effect on the treatment of asthma exacerbation (Aliyali et al., 2010), carbocisteine reduces the cough reflex in asthmatic patients (Ishiura et al., 2003). Thus, L-carbocisteine may have clinical benefits in the management of bronchial asthma and COPD.

In summary, this is the first report that a mucolytic agent, L-carbocisteine, inhibits RS virus infection and decreases the susceptibility of cultured human tracheal epithelial cells to RS virus infection by reducing levels of ICAM-1, a RS virus receptor. L-carbocisteine also reduced the baseline and RS virus infection-induced secretion of pro-inflammatory cytokines, including IL-1β, IL-6 and IL-8. L-carbocisteine may modulate airway inflammation after RS virus infection.

Conflicts of interest

We declare no conflicts of interest.

References

Aliyali, M., Poorhasan Amiri, A., Sharifpoor, A., Zalli, F., 2010. Effects of N-acetylcysteine on asthma exacerbation. Iran. J. Allergy Asthma Immunol. 9, 103–109.

Asada, M., Yoshida, M., Suzuki, T., Hatachi, Y., Sasaki, T., Yasuda, H., Nakayama, K., Nishimura, H., Nagatomi, R., Kubo, H., Yamaya, M., 2009. Macrolide antibiotics inhibit respiratory syncytial virus infection in human airway epithelial cells. Antiviral Res. 83, 191–200.

Behera, A.K., Matsuse, H., Kumar, M., Kong, X., Lockey, R.F., Mohapatra, S.S., 2001. Blocking intercellular adhesion molecule-1 on human epithelial cells decreases respiratory syncytial virus infection. Biochem. Biophys. Res. Commun. 280, 188–195.

Budge, P.J., Lebowitz, J., Graham, B.S., 2003. Antiviral activity of RhoA-derived peptides against respiratory syncytial virus is dependent on formation of peptide dimmers. Antimicrob. Agents Chemother. 47, 3470–3477.

Chikumi, H., Fukuhara, S., Gutkind, J.S., 2002. Regulation of G protein-linked guanine nucleotide exchange factors for Rho, PDZ-RhoGEF, and LARG by tyrosine phosphorylation: evidence of a role for focal adhesion kinase. J. Biol. Chem. 277, 12463–12473.

Collins, P.L., Crowe Jr., J.E., 2006. Respiratory syncytial virus and metapneumovirus. In: Knipe, D.M., Howley, P.M. (Eds.), Fields Virology., 5th ed. Lippincott Williams & Wilkins, Philadelphia, pp. 1601–1646.

Condit, R.C., 2006. Principles of virology. In: Knipe, D.M., Howley, P.M. (Eds.), Fields Virology., 5th ed. Lippincott Williams & Wilkins, Philadelphia, pp. 25–57.

Dechecchi, M.C., Melotti, P., Bonizzato, A., Santacatterina, M., Chilosi, M., Cabrini, G., 2001. Heparan sulfate glycosaminoglycans are receptors sufficient to mediate the initial binding of adenovirus types 2 and 5. J. Virol. 75, 8772–8780.

De Schutter, J.A., Van der Weken, G., Van den Bossche, W., de Moerloose, P., 1988. Determination of S-carbomethylcysteine in serum by reversed-phase ion-pair liquid chromatography with column switching following pre-column derivatization with o-phtalaldehyde. J. Chromatogr. B 428, 301–310.

Feldman, S.A., Hendry, R.M., Beeler, J.A., 1999. Identification of a linear heparin binding domain for human respiratory syncytial virus attachment glycoprotein G. J. Virol. 73, 6610–6617.

Guidry, G.G., Black-Payne, C.A., Payne, D.K., Jamison, R.M., George, R.B., Bocchini Jr., J.A., 1991. Respiratory syncytial virus infection among intubated adults in a university medical intensive care unit. Chest 100, 1377–1384.

Hallak, L.K., Collins, P.L., Knudson, W., Peeples, M.E., 2000. Iduronic acid-containing glycosaminoglycans on target cells are required for efficient respiratory syncytial virus infection. Virology 271, 264–275.

Hayden, F.G., Gwaltney Jr., J.M., 1988. Viral infections. In: Murray, J., Nadel, J.A. (Eds.), Textbook of Respiratory Medicine. Saunders, Philadelphia, pp. 748–802.

Hegab, A.E., Kubo, H., Yamaya, M., Asada, M., He, M., Fujino, N., Mizuno, S., Nakamura, T., 2008. Intranasal HGF administration ameliorates the physiologic and morphologic changes in lung emphysema. Mol. Ther. 16, 1417–1426.

Henderson, F.W., Clyde Jr., W.A., Collier, A.M., Denny, F.W., Senior, R.J., Sheaffer, C.I., Conley 3rd, W.G., Christian, R.M., 1979. The etiologic and epidemiologic spectrum of bronchiolitis in pediatric practice. J. Pediatr. 95, 183–190.

Iesato, K., Tatsumi, K., Saito, K., Ogasawara, T., Sakao, S., Tada, Y., Kasahara, Y., Kurosu, K., Tanabe, N., Takiguchi, Y., Kuriyama, T., Shirasawa, H., 2008. Tiotropium bromide attenuates respiratory syncytial virus replication in epithelial cells. Respiration 76, 434–441.

Ishiura, Y., Fujimura, M., Yamamori, C., Nobata, K., Myou, S., Kurashima, K., Michishita, Y., Takegoshi, T., 2003. Effect of carbocisteine on cough reflex to capsaicin in asthmatic patients. Br. J. Clin. Pharmacol. 55, 504–510.

Kadowaki, S., Chikumi, H., Yamamoto, H., Yoneda, K., Yamasaki, A., Sato, K., Shimizu, E., 2004. Down-regulation of inducible nitric oxide synthase by lysophosphatidic acid in human respiratory epithelial cells. Mol. Cell Biochem. 262, 51–59.

Mills, G.B., Moolenaar, W.H., 2003. The emerging role of lysophosphatidic acid in cancer. Nat. Rev. 3, 582–591.

Narumiya, S., 1996. The small GTPase Rho: cellular functions and signal transduction. J. Biochem. 120, 215–228.

Noah, T.L., Becker, S., 1993. Respiratory syncytial virus-induced cytokine production by a human bronchial epithelial cell line. Am. J. Physiol. 265, L472–L478.

Numazaki, Y., Oshima, T., Ohmi, A., Tanaka, A., Oizumi, Y., Komatsu, S., Takagi, T., Karahashi, M., Ishida, N., 1987. A microplate method for isolation of viruses from infants and children with acute respiratory infections. Microbiol. Immunol. 31, 1085–1095.

Pastey, M.K., Crowe Jr., J.E., Graham, B.S., 1993. RhoA interacts with the fusion glycoprotein of respiratory syncytial virus and facilitates virus-induced syncytium formation. J. Virol. 73, 7262–7270.

Pastey, M.K., Gower, T.L., Spearman, P.W., Crowe Jr., J.E., Graham, B.S., 2000. A RhoA-derived peptide inhibits syncytium formation induced by respiratory syncytial virus and parainfluenza virus type 3. Nat. Med. 6, 35–40.

Raats, C.J., Bakker, M.A., van den Born, J., Berden, J.H., 1997. Hydroxyl radicals depolymerize glomerular heparan sulfate in vitro and in experimental nephrotic syndrome. J. Biol. Chem. 272, 26734–26741.

Takai, Y., Sasaki, T., Matozaki, T., 2001. Small GTP-binding proteins. Physiol. Rev. 81, 153–208.

Tatsumi, K., Fukuchi, Y., PEACE Study Group, 2007. Carbocisteine improves quality of life in patients with chronic obstructive pulmonary disease. J. Am. Geriatr. Soc. 55, 1884–1886.

Tripp, R.A., Oshansky, C., Alvarez, R., 2005. Cytokines and respiratory syncytial virus infection. Proc. Am. Thorac. Soc. 2, 147–149.

Wu, A., Pangalos, M.N., Efthimiopoulos, S., Shioi, J., Robakis, N.K., 1997. Appican expression induces morphological changes in C6 glioma cells and promotes adhesion of neural cells to the extracellular matrix. J. Neurosci. 17, 4987–4993.

Yamaguchi, Y., Katoh, H., Yasui, H., Mori, K., Negishi, M., 2001. RhoA inhibits the nerve growth factor-induced Rac1 activation through Rho-associated kinase-dependent pathway. J. Biol. Chem. 276, 18977–18983.

Yamaya, M., Nishimura, H., Hatachi, Y., Yoshida, M., Fujiwara, H., Asada, M., Nakayama, K., Yasuda, H., Deng, X., Sasaki, T., Kubo, H., Nagatomi, R., 2011. Procaterol inhibits rhinovirus infection in primary cultures of human tracheal epithelial cells. Eur. J. Pharmacol. 650, 431–444.

Yasuda, H., Yamaya, M., Sasaki, T., Inoue, D., Nakayama, K., Tomita, N., Yoshida, M., Sasaki, H., 2006a. Carbocisteine reduces frequency of common colds and exacerbations in COPD patients. J. Am. Geriatr. Soc. 54, 378–380.

Yasuda, H., Yamaya, M., Sasaki, T., Inoue, D., Nakayama, K., Yamada, M., Suzuki, T., Sasaki, H., 2006b. Carbocisteine inhibits rhinovirus infection in human tracheal epithelial cells. Eur. Respir. J. 28, 51–58.

Zheng, J.P., Kang, J., Huang, S.G., Chen, P., Yao, W.Z., Yang, L., Bai, C.X., Wang, C.Z., Wang, C., Chen, B.Y., Shi, Y., Liu, C.T., Chen, P., Li, Q., Wang, Z.S., Huang, Y.J., Luo, Z.Y., Chen, F.P., Yuan, J.Z., Yuan, B.T., Qian, H.P., Zhi, R.C., Zhong, N.S., 2008. Effect of carbocisteine on acute exacerbation of chronic obstructive pulmonary disease (PEACE study): a randomised placebo-controlled study. Lancet 371, 2013–2018.

Sleep Medicine 13 (2012) 831–837

Contents lists available at SciVerse ScienceDirect

Sleep Medicine

journal homepage: www.elsevier.com/locate/sleep

Original Article

The association between sleep problems and perceived health status: A Japanese nationwide general population survey

Ryuji Furihata [a], Makoto Uchiyama [a,*], Sakae Takahashi [a], Masahiro Suzuki [a], Chisato Konno [a], Kouichi Osaki [a], Michiko Konno [a], Yoshitaka Kaneita [b], Takashi Ohida [b], Toshiki Akahoshi [c], Shu Hashimoto [c], Tsuneto Akashiba [c,d]

[a] Department of Psychiatry, Nihon University School of Medicine, Tokyo, Japan
[b] Division of Public Health, Department of Social Medicine, Nihon University School of Medicine, Tokyo, Japan
[c] Division of Respiratory Medicine, Department of Internal Medicine, Nihon University School of Medicine, Tokyo, Japan
[d] Division of Sleep Medicine, Department of Internal Medicine, Nihon University School of Medicine, Tokyo, Japan

ARTICLE INFO

Article history:
Received 13 September 2011
Received in revised form 2 March 2012
Accepted 7 March 2012
Available online 19 May 2012

Keywords:
Perceived health status
Epidemiology
Sleep
Insomnia
Quality of life
Japan

ABSTRACT

Objective: Sleep problems in humans have been reported to impact seriously on daily function and to have a close association with well-being. To examine the effects of individual sleep problems on physical and mental health, we conducted a nationwide epidemiological survey and examined the associations between sleep problems and perceived health status.
Methods: Cross-sectional surveys with a face-to-face interview were conducted in August and September, 2009, as part of the Nihon University Sleep and Mental Health Epidemiology Project (NUSMEP). Data from 2559 people aged 20 years or older were analyzed (response rate 54.0%). Participants completed a questionnaire on perceived physical and mental health statuses, and sleep problems including the presence or absence of insomnia symptoms (i.e., difficulty initiating sleep [DIS], difficulty maintaining sleep [DMS], and early morning awakening [EMA]), excessive daytime sleepiness (EDS), poor sleep quality (PSQ), short sleep duration (SSD), and long sleep duration (LSD).
Results: The prevalence of DIS, DMS, and EMA was 14.9%, 26.6%, and 11.7%, respectively, and 32.7% of the sample reported at least one of them. At the complaint level, the prevalence of EDS, PSQ, SSD, and LSD was 1.4%, 21.7%, 4.0%, and 3.2%, respectively. Multiple logistic regression analyses revealed that DMS, PSQ, SSD, and LSD were independently associated with poor perceived physical health status; DIS, EDS, and PSQ were independently associated with poor perceived mental health status.
Conclusions: This study has demonstrated that sleep problems have individual significance with regard to perceived physical or mental health status.

1. Introduction

Insomnia has been recognized as one of the most common difficulties in modern society. Epidemiological studies have reported that the prevalence of insomnia symptoms in the general population ranges from 17.3% to 48% [1–3] and is consistent when the insomnia criteria used are comparable.

The restorative function of sleep is undoubtedly essential for maintenance of both physical and mental health. Previous studies in several countries have indicated that insomnia is associated with perceived health [4–20]. Léger et al. [15] reported that the severity of insomnia was correlated with perceived health, and Hajak [12] found that impairment of perceived health in individuals with severe insomnia was somewhat greater than that in individuals with long-standing physical illness.

Apart from insomnia, excessive daytime sleepiness (EDS) [9,17], short sleep duration (SSD) [18,21–23], long sleep duration (LSD) [18,21,23], and poor sleep quality (PSQ) [24] have also been associated with poor perceived health.

Several studies have suggested that sleep problems disturb both perceived physical and mental health [8,9,12,14–16], while recently it has been suggested that sleep problems have different effects on physical and mental health [11,17,20]. A cross-sectional study of older women suggested that sleep difficulty was significantly associated with poor perceived mental health, but not with poor perceived physical health [11]. A study of hypnotic medication use suggested that this was associated with deterioration of

* Corresponding author. Address: Department of Psychiatry, Nihon University School of Medicine, Oyaguchi-kamicho, 30-1 Itabashi-ku, Tokyo 173-8610, Japan. Tel.: +81 3 3972 8111x2431; fax: +81 3 3972 2920.
E-mail address: uchiyama.makoto@nihon-u.ac.jp (M. Uchiyama).

1389-9457/$ - see front matter © 2012 Elsevier B.V. All rights reserved.
http://dx.doi.org/10.1016/j.sleep.2012.03.011

physical health, but not mental health [20]. A retrospective study found that insomnia was associated with changes in perceived mental health, but not with changes in perceived physical health [17].

With regard to the association between sleep problems and perceived health, most previous studies did not focus on the subtypes of sleep problems, i.e., difficulty initiating sleep (DIS), difficulty maintaining sleep (DMS), or early morning awakening (EMA). More recently, a 3-year follow-up study of an elderly population demonstrated that sleep-onset insomnia, but not other subtypes of insomnia, was a risk factor for depression [25]. A 12-year follow-up study of community-dwelling adults showed that sleep-maintenance insomnia, but not other subtypes, was a significant risk factor for the development of type 2 diabetes mellitus, suggesting that the consequences of various insomnia subtypes may differ [26]. Furthermore, few previous studies selected subjects from the general adult population; in most cases, the subjects were selected from a particular age group or community.

Here we conducted an epidemiological study of sleep problems and perceived health status in a large sample of the Japanese general adult population. We investigated the associations between sleep problems and perceived physical and mental health status, focusing on sleep problem subtypes. Our particular interest was focused on the associations of individual sleep problems with perceived physical and mental health statuses by adjusting for confounding relationships.

2. Methods

2.1. Selection of subjects

The Nihon University Sleep and Mental Health Epidemiology Project (NUSMEP) was conducted in August and September, 2009. This study was part of an omnibus survey commissioned to a polling agency. A three-stage stratified sampling method was used. Municipalities were stratified into 31 units representing 12 geographical blocks and three types of city scale (metropolises, other cities, and towns and villages) in proportion to the population distribution in 2008. At the first stage, the target unit was randomly selected from 31 units. At the second stage, a total of 8000 houses were randomly selected from a digital house map of each target unit. At the third stage, the interviewer visited the houses and found that residents were present in 4738 of them. An individual aged 20 years or older was randomly selected from each house. Finally 2559 individuals gave oral informed consent and participated in the survey (response rate 54.0%), completing a face-to-face interview with a trained interviewer by reference to a panel-listed structural questionnaire. For the present report, we obtained the electronic data file for the relevant interview component, with no personal identifiers.

The study was approved by the ethics committee of the Nihon University School of Medicine.

2.2. Procedures

2.2.1. Perceived physical and mental health statuses

Perceived physical health status was assessed with the question: "What do you think about your physical health status?" ("very sufficient," "sufficient," "normal," "insufficient," or "very insufficient"). Perceived mental health status was assessed with the question: "What do you think about your mental health status?" ("very sufficient", "sufficient", "normal", "insufficient", or "very insufficient"). For each question, the responses "insufficient" and "very insufficient" were considered to indicate "poor perceived physical or mental health status", and "normal", "sufficient", and "very sufficient" were considered to indicate "good perceived physical or mental health status", thus dichotomizing the responses for multiple logistic regression analysis.

2.2.2. Sleep problems

We drew up seven questions that allowed us to infer patterns of sleep disturbance in the subjects, with reference to the Japanese version of the Pittsburgh Sleep Quality Index (PSQI) [27,28]. The following questions about sleep experienced during the previous month were included in the questionnaire:

1. How often have you had difficulty falling asleep? ("not at all," "less than once a week," "once or twice a week," or "three or more times a week"): difficulty initiating sleep (DIS).
2. How often have you woken up frequently at night? ("not at all," "less than once a week," "once or twice a week," or "three or more times a week"): difficulty maintaining sleep (DMS).
3. How often have you woken up too early in the morning? ("not at all," "less than once a week," "once or twice a week," or "three or more times a week"): early morning awakening (EMA).
4. How often have you had trouble staying awake while driving, eating meals, or engaging in social activity? ("not at all," "less than once a week," "once or twice a week," or "three or more times a week"): excessive daytime sleepiness (EDS).
5. How often have you taken medicine to help you sleep (prescribed or "over the counter")? ("not at all," "less than once a week," "once or twice a week," or "three or more times a week"): hypnotic medication use.
6. How do you rate your sleep quality overall? ("very good," "fairly good," "fairly bad," or "bad"): poor sleep quality (PSQ).
7. How many hours of actual sleep do you get at night?: sleep duration.

For questions 1–4, participants who answered "once or twice a week," or "three or more times a week" were classified as having symptoms.

For question 5, participants who answered "less than once a week", "once or twice a week," or "three or more times a week" were classified as "taking hypnotic medication."

For question 6, participants who answered "fairly bad" or "bad" were classified as having "PSQ".

For question 7, participants who answered "less than 5 h" were categorized as having "short sleep duration (SSD)" and those who answered "more than 9 h" were categorized as having "long sleep duration (LSD)."

2.2.3. Sociodemographic characteristics

Variables analyzed included gender, age, educational achievement, marital status, and city scale. Age was divided into three groups: 20–39 years, 40–59 years, and 60 years of age and older. Educational achievement was divided into three groups: junior high school, senior high school, and college or higher. Marital status was divided into two groups: married and unmarried. City scale was divided into three groups: metropolises, other cities, and towns and villages.

2.3. Statistical analysis

Gender and age differences for the prevalence ratio obtained in the present study were examined using χ^2 test. Multiple logistic regression analyses were utilized to examine the associations between poor perceived physical or poor perceived mental health status and the number of insomnia symptoms. Finally, a series of logistic regression analyses was conducted to examine the association between poor perceived physical health status or poor

perceived mental health status and sleep problems (DIS, DMS, EMA, EDS, PSQ, SSD, and LSD). After conducting crude logistic regression analyses, we carried out multiple logistic regression analyses to adjust for confounding effects of sociodemographic variables, and for confounding effects of sociodemographic variables and other sleep problems. Odds ratios (ORs) and 95% confidence intervals (95% CI) were calculated for the series of logistic regression analyses. All analyses were performed using SPSS 19.0 for Windows.

3. Results

Table 1 shows the gender and age distribution of the study participants and the total population, along with the corresponding population distributions estimated from 2008 data [29]. The distributions of the present study sample seemed similar to those estimated for the Japanese general adult population.

The proportions of participants having poor perceived physical health status and poor perceived mental health status were sorted by gender and age (Table 2). There was no apparent gender difference in the proportion of participants claiming to have poor perceived physical health status or poor perceived mental health status (poor perceived physical health status $\chi^2 = 0.27$, df = 1, $P = 0.61$, poor perceived mental health status $\chi^2 = 0.89$, df = 1, $P = 0.77$). The prevalence of poor perceived physical health status seemed to increase with age, and there was a significant age effect for both men and women (men $\chi^2 = 76.0$, df = 5, $P < 0.01$, women $\chi^2 = 87.9$, df = 5, $P < 0.01$).

Table 3 shows the prevalence of sleep problems by gender and age, 95% CIs, and the results of the χ^2 tests. The prevalence of DIS, DMS, and EMA was 14.9%, 26.6%, and 11.7%, respectively, and the prevalence of any insomnia symptom was 32.7%. The prevalence of EDS, PSQ, SSD, and LSD was 1.4%, 21.7%, 4.0%, and 3.2%, respectively. The prevalence of DIS and DMS was significantly higher in women than in men. The prevalence of DMS, EMA, PSQ, and sleep duration differed significantly among the age groups in both men and women.

The prevalence of poor perceived physical health status and that of poor perceived mental health status increased significantly with the number of insomnia symptoms the subject had (Table 4). Multiple logistic regression analyses revealed a significant "dose effect" of the number of insomnia symptoms on both poor perceived physical and mental health statuses after adjustment for sociodemographic factors.

Multiple logistic regression analyses demonstrated that DMS, PSQ, SSD, and LSD were associated with an increased OR for poor perceived physical health status after adjusting for sociodemographic variables and other sleep problems (Table 5).

Multiple logistic regression analyses demonstrated that DIS, EDS, and PSQ were associated with an increased OR for poor perceived mental health status after adjustment for sociodemographic variables and other sleep problems (Table 6).

Table 1
Percentage of study participants and the general population classified according to gender and age.

Age (year)	Present study (2009)		Population estimates (2008)	
	Men (%)	Women (%)	Men (%)	Women (%)
20–29	14.1	11.0	15.0	13.3
30–39	18.7	16.8	18.7	17.0
40–49	17.6	15.7	16.2	14.9
50–59	16.0	18.0	17.4	16.4
60–69	17.6	19.1	16.3	16.2
70+	15.9	19.6	16.3	22.2
Total	100.0	100.0	100.0	100.0
n	1163	1396	50,295 (thousands)	54,064 (thousands)

4. Discussion

This report represents one of the first attempts to investigate the association between sleep problems and perceived physical and mental health statuses among the Japanese general adult population. The major findings of this study were: (1) the number of insomnia symptoms was associated with increased odds ratios for poor perceived physical or mental health status; (2) DMS, PSQ, SSD, and LSD were independently associated with poor perceived physical health status; (3) DIS, EDS, and PSQ were independently associated with poor perceived mental health status.

4.1. Prevalence of poor perceived physical or mental health status

In the present study the prevalence of poor perceived physical health status increased significantly with age, while that of poor perceived mental health status did not differ across age groups. Previous studies have demonstrated that perception of physical health declines with advanced age [30–34]. Previous studies did not demonstrate any effect of age on mental health condition [31,35] and, in fact, mental health tended to be better in the aged than in younger groups [33,34]. These results may be interpreted to reflect age-related physical decline or an increase of comorbid disorders, whereas perceived mental health is not age-dependent. Thus, the present epidemiological data for perceived physical and mental health status are comparable with those of previous studies.

No gender difference was found in the prevalence of poor perceived physical or mental health status in the present study. As for gender difference in perceived health, findings reported in the previous studies appeared to be conflicting. Several studies have reported no gender difference in perceived mental and physical health [10,35], while others have suggested that a gender difference exists in this respect [17,20,33,34,36,37]. This inconsistency may be due in part to differences in the methodology used for evaluating perceived health, i.e., definition, duration, and setting. Further studies are needed to verify these findings.

4.2. Prevalence of insomnia

In the present study the overall prevalence of insomnia was 32.7%, which was comparable to the findings of previous epidemiological studies [1–3]. Our study showed that the prevalence of insomnia increased with age. Previous studies have also found that the prevalence of insomnia is higher in the elderly than in younger or middle-aged individuals [1,38,39]. Such age-dependent increases in the prevalence of insomnia appear to be more marked with respect to DMS and EMA. Our study showed that the overall prevalence of insomnia was higher in women than in men, thus being comparable with previous reports [6,12,38,40,41]. As for the subtypes of insomnia, gender differences were more evident for DIS and DMS, while EMA showed no significant gender difference. Similar features have been demonstrated in epidemiological studies conducted in Asian and Western countries [4,42–44].

4.3. Number of insomnia symptoms and poor perceived health status

In the present study, using multiple logistic regression analyses, we investigated the association between the number of insomnia symptoms and perceived health status, and found "dose effects" of insomnia symptoms on the prevalence of poor perceived health